Seascape genetic study on Laminaria digitata underscores the critical role of sampling schemes

Louise Fouqueau, L Reynes, F Tempera, T Bajjouk, A Blanfuné, C Chevalier, M Laurans, S Mauger, M Sourisseau, J Assis, et al.

Seascape genetic study on *Laminaria digitata* underscores the critical role of sampling schemes

Fouqueau L.[1,∝,*], Reynes L.[1], Tempera F.[2], Bajjouk T.[2], Blanfuné A.[3], Chevalier C.[3], Laurans M.[4], Mauger S.[1], Sourisseau M. [2], Assis J.[5,6], Lévêque L.[7], Valero M.[1]

[1] IRL 3614, CNRS, Sorbonne Université, Pontificia Universidad Católica de Chile, Universidad Austral de Chile, Station Biologique de Roscoff, 29688 Roscoff, France; [2] Dynamic of Coastal Ecosystems, DYNECO, Ifremer, Technopôle Brest Iroise, Plouzané 29280, France; [3] Aix-Marseille Université, Université de Toulon, CNRS, IRD, MIO, 13288 Marseille, France; [4] LBH-Halgo-DECOD, Ifremer, Centre de Bretagne, 29280 Plouzané, France; [5] CCMAR, University of the Algarve, 8005-139 Faro, Portugal; [6] Faculty of Bioscience and Aquaculture, Nord Universitet, 1490 Bodø, Norway; [7] FR2424, CNRS, Sorbonne Université, Station Biologique de Roscoff, 29688 Roscoff, France.

[∝] Present address: Institute of Science and Technology Austria, 3400 Klosterneuburg, Austria.

[*] Corresponding author: louise.fouqueau@ist.ac.at.

SHORT TITLE: Seascape genetic study on *Laminaria digitata*

ABSTRACT:

Understanding connectivity patterns in endangered species living in fragmented habitats is fundamental to improve management and conservation actions. Such improvements can be particularly pressing at trailing edges where populations are facing the greatest challenges of climate change, and appear all the more crucial if the species is commercially harvested. Seascape genetics have been increasingly used to meet these needs. In this study, we examined connectivity patterns among 32 populations located at the southern range limit of the oarweed kelp *Laminaria digitata*. Our populations were sampled in a roughly continuous manner, with the distance between neighboring populations ranging from a few km to about a few hundreds. By genotyping 11 microsatellite markers, our aim was to (1) refine analyses of population structure, (2) test whether on-shelf islands are genetically more differentiated compared to mainland populations, (3) evaluate the relative importance of various abiotic conditions in shaping the genetic structure and (4) evaluate if the relative importance of each environmental factor varied according to sampling schemes. Our analyses revealed a positive relation between connectivity links and genetic diversity: populations with high levels of connectivity were genetically enriched while isolated populations showed signs of genetic erosion. The genetically impoverished populations corresponded to the southernmost populations as well as populations along the northern coast of Brittany (Locquirec, Saint-Malo Bay) and the northernmost population in Pas-de-Calais. By performing db-RDA on various sampling schemes, geographic distance appeared as the dominant factor influencing connectivity between populations separated by great distances, while hydrodynamic processes were the main factor when analyzing continuously distributed populations.

KEYWORDS: connectivity, seascape genetics, *Laminaria digitata*, microsatellite markers, sampling scheme

1. INTRODUCTION

Understanding connectivity patterns in endangered species living in fragmented habitats is fundamental to assess their vulnerability to environmental changes and to define conservation measures at appropriate scales (Manel et al. 2019, Benestan et al. 2023). Such knowledge is particularly relevant at the trailing edge of species distribution, where the numerous effects of global warming can interfere with the strong genetic and demographic drifts (Nadeau & Urban 2019). Investigating connectivity can additionally pinpoint populations that are isolated from gene flow. Yet genetic isolation can, in some cases, impede adaptation and ultimately lead to extinction (Lynch & Lande 1993). A deeper understanding of population connectivity can therefore advance conservation action aiming to preserve species adaptive potential via measures that prevent the loss of genetic diversity.

Most marine organisms disperse through planktonic propagules (*e.g.*, spores, eggs, larvae) which are deemed unable to counter hydrodynamic forces (Alberto et al. 2010). The influence of oceanographic processes on population genetic structure has therefore been repeatedly proven in different marine taxa by means of biophysical models (*e.g.*, Gilg & Hilbish 2003, Treml et al. 2008, Mitarai et al. 2009 and more recently by Xuereb et al. 2018, Benestan et al. 2021, Reynes et al. 2021). For instance, hydrodynamic processes have been associated with larval retention and asymmetrical gene flow (Gaylord & Gaines 2000), both of which inevitably affect metapopulation dynamics. White et al. (2010) have additionally demonstrated that ocean currents enable exchanges between coastal islands - defined as the ones located on the continental shelf - and mainland populations. Although coastal islands have limited evolutionary and ecological interests compared to more remote oceanic islands (Dawson 2016), understanding their connectivity patterns could still have significant implications for conservation. Yet, to this date, a formal comparison of the connectivity between on-shelf island and coastal populations is still lacking for marine species in comparison to terrestrial ones (Bell 2008). Although oceanic currents are fundamental in shaping the genetic structure of marine species, their effects on their own are insufficient to explain entire connectivity patterns (Hu et al. 2020). Species' life history traits and larval behavior appear to

influence dispersal kernels to a certain extent (Sanford & Kelly 2011), as illustrated by the differences in phylogeographic breaks among marine taxa, albeit historical patterns and/or habitat availability being also at play (Teske et al. 2011, 2017, Martins et al. 2022). When considering heterogeneous environments, local adaptation can constrain gene flow (or the rate of effective migration, Aeschbacher et al. 2017) even in the absence of physical barriers to dispersal, a phenomenon that has been termed "isolation by adaptation" (Nosil et al. 2009, Schoville et al. 2012). In such scenarios, contrasted patterns of genetic structure can be observed at neutral and putatively selected loci (see Grummer et al. 2019 for review and Sandoval-Castillo et al. 2018, Van Oppen & Coleman 2022).

Seascape genetics aims to investigate which and how marine environmental features influence the spatial distribution of genetic variation at neutral or putatively adaptive loci (Xuereb et al. 2019, Boussarie et al. 2022). Among the tested features, water depth (*e.g.*, Engel et al. 2004, Hickey et al. 2009, Krueger-Hadfield et al. 2013), habitat discontinuity (*e.g.*, Alberto et al. 2010, 2011, D'Aloia et al. 2014, Durrant et al. 2018), sea surface temperature ("SST", *e.g.*, Johansson et al. 2015, Benestan et al. 2016, Guzinski et al. 2020) and salinity (*e.g.*, Gaggiotti et al. 2009, Sjöqvist et al. 2015) have been shown to explain, separately or jointly, a large part of the variation in genetic structure. However, most of these studies have relied on linear regressions and Mantel tests to show the influence of environmental factors (see Benestan et al. 2016 for references), although these statistical frameworks suffer from high false positive rates (Graves et al. 2013). This problem has been significantly reduced by the use of variance partitioning methods (Capblancq & Forester 2021), such as distance-based redundancy analysis (db-RDA; Legendre & Anderson 1999). In addition to the statistical advances, the improvement of hydrodynamic models and the developments of Moran's and asymmetric eigenvector maps (Dray et al. 2006, Blanchet et al. 2008b) allowed a better apportioning of the contribution of geographic distance and oceanographic features (*e.g.*, Benestan et al. 2016, 2021, Xuereb et al. 2018, Reynes et al. 2021). Yet some of the oceanographic processes have very localized effects (Legendre & Demers 1984), and other abiotic factors influencing genetic structure (*e.g.*, SST) can similarly vary at a fine

geographical scale (see for example Gallon et al. 2014). Their relative influence on genetic structure is therefore expected to vary according to geographical extents (Jombart et al. 2009, Dalongeville et al. 2018), which underlines how sampling design can itself influence the conclusions.

Kelp forests are a dominant feature along many temperate to boreal rocky shores and play a foundation role for numerous species by providing them substrate, shelter or food (Teagle et al. 2017, Jayathilake & Costello 2020, Coleman & Veenhof 2021). The decline they have shown in some North-East Atlantic biogeographic regions has justified their recent inclusion in the OSPAR list of threatened and declining habitats (de Bettignies et al. 2021). SST is considered as the major abiotic factor shaping kelp species' distribution as denoted by the cold-water niches they tend to associate with (Lüning 1990, Bartsch et al. 2008). Over the past decade, various studies have shown the harmful consequences of rising SST on kelp forests, notably as a result of ever more frequent and intense marine heatwaves , which especially affect warm-edge populations (Fernández 2011, Starko et al. 2019, Arafeh-Dalmau et al. 2019, Filbee-Dexter et al. 2020, but see Klingbeil et al. 2022). In this context, clarifying connectivity in the warm distribution edge might be particularly valuable to gauge the resilience of marginal populations. For instance, detecting effective dispersal from the range center towards the margin could indicate the possibility of an evolutionary rescue. Yet, an evolutionary rescue will be possible only if marginal and core populations are adapted to similar environmental conditions (Bridle et al. 2009, DuBois et al. 2022).

Laminaria digitata (Hudson) J.V. Lamouroux is a boreal kelp species with an amphi-Atlantic distribution. Its geographic range in the northeast Atlantic extends from temperate southern Brittany (47ºN, France) to the arctic Spitsbergen archipelago (79ºN, Norway) (Kain 1979, Lüning 1990, Araújo et al. 2016). Along the shorelines, *L. digitata* generally occurs within a narrow band spanning the lower intertidal and upper subtidal zones (Robuchon et al. 2014). This species thus presents an interesting case to test the effect of coastal oceanographic currents on genetic structure, especially along the rugged coast of Brittany, where hydrodynamics is highly complex due to

numerous mesoscale features (*e.g.*, fronts, upwellings, river plumes, low salinity lenses) and macrotidal ranges (Salomon & Breton 1993, Ayata et al. 2010, Nicolle et al. 2017). This species has been historically harvested in Brittany, where an adaptation of the ongoing exploitation is currently under discussion (Garineaud 2021). Additionally, annual mean SST varies at a fine scale across Brittany, with the western and north-western sectors being cooler and currently less affected by climate change than Southern and North-Eastern Brittany (Gallon et al. 2014). As suggested by Liesner et al. (2020), this mosaic of SST conditions might have driven the distinct thermal adaptations observed between populations from northern and southern Brittany. Finally, by using a hierarchical sampling scheme, previous analyses of population structure at the scale of Brittany have revealed significant genetic differentiation at both small (< 1 km) and large scales (> 10-50 km) relative to the region (Billot et al. 2003, Robuchon et al. 2014).

In this study, we extended the geographical sampling of previous microsatellite analyses (Billot et al. 2003, Valero et al. 2011, Couceiro et al. 2013, Robuchon et al. 2014) by using a dataset built from 32 populations ranging from the southern range limit of *L. digitata* to the northernmost population found on the French coast, situated in the Strait of Dover. Using this dataset, we explored the respective and combined effects of sampling year, hydrodynamic processes, habitat discontinuity, spatial distance and SST on the genetic structure. We specifically aimed to (1) refine the previous analyses of population structure for this species and identify isolated populations, (2) test whether on-shelf island populations are genetically more differentiated compared to mainland populations and thus show signs of genetic erosion, (3) evaluate the relative importance of each environmental factor in shaping the genetic structure using a db-RDA and finally (4) evaluate if their relative importance varies according to the sampling scheme.

2. MATERIAL AND METHODS

2.1. Study area

Brittany is the northwestern-most region of mainland France (NE Atlantic, Figure 1). Its 2,860 km-length coastline encompasses a major biogeographical transition zone between cold- and

156 warm-temperate waters (Spalding et al. 2007). The northern shores, which border the English
157 Channel, are characterized by well-mixed waters produced by a macrotidal regime that intensifies
158 eastwards. Contrastingly, waters in southern Brittany are seasonally to permanently stratified and
159 show larger temperature fluctuations throughout the year (Gallon et al. 2014, Blauw et al. 2019).
160 Brittany's western-most sector is subject to both the macrotidal regime and the full impact of
161 Atlantic storms, which collectively maintain well-mixed conditions throughout the year and curb
162 seasonal temperature fluctuations (Gallon et al. 2014). Various boreal-affinity species benefit from
163 this nutrient-rich and thermally-buffered environment, including various kelp species that form
164 some of Europe's most important marine forests along Brittany's rocky shores.

165 2.2. Samples

166 Populations of *Laminaria digitata* were sampled between 2003 and 2015 in 32 sites ranging from
167 the southern limit of its NE Atlantic distribution (47°N) up to the Strait of Dover, at the entrance
168 of the North Sea (50°N, Table 1, Figure 1). The population at the Strait of Dover (S32) is known
169 to be geographically isolated, with the closest population along the French coast being in Étretat,
170 at *circa* 200 km to the southwest (see Figure 2C of Araújo et al. 2016) and for which we did not
171 have any sample. Among our populations, 10 were located around islands while 22 were on the
172 mainland coast (Table 1, Figure 1). In our study, we have defined *island* populations as those
173 situated on the continental shelf (*i.e.*, above 200 m depth, Dawson 2016). All of them were part of
174 the mainland during the Last Glacial Maximum when the ocean level was approximately 120 m
175 lower than present (Figure 1, Frenzel et al. 1992, Lambeck 1997). Some of these populations were
176 sampled and genotyped for previous studies as indicated in Table 1. At each site, blade tissue was
177 collected from 30 to 50 randomly selected sporophytes. Tissue samples were then wiped, cleaned
178 from epiphytes and stored in silica-gel crystals until DNA extraction.

179 2.3. Microsatellite genotyping

180 2.3.1. DNA extraction

181 DNA was extracted from 8–12 mg of dried tissue using the NucleoSpin 96 Plant II kit (Macherey-
182 Nagel GmbH & Co. KG) following manufacturer's instructions. The lysis, microsatellite

amplification and scoring were performed for 12 polymorphic loci following Robuchon et al. (2014). Multiplex PCRs were modified using 5X GoTaq Flexi colorless reaction buffer (Promega Corp., Madison, USA) instead of 1X and performed using a T100™ Thermal Cycler (Bio-Rad Laboratories Inc.).

2.3.2. Microsatellite amplification, scoring

Among the markers used for this study, six were developed for *L. digitata* (Ld148, Ld158, Ld167, Ld371, Ld531, and Ld704; Billot et al. 1998) and five for *L. ochroleuca* (Lo4-24, Lo454-17, Lo454-23, Lo454-24, and Lo454-28; Coelho et al. 2014). Alleles were sized using the SM594 size standard (Mauger et al. 2012) and scored manually using GeneMapper 4.0 (Applied Biosystems). Individuals for which more than one locus did not amplify were removed from the dataset.

2.4. Preliminary analyses

Prior to genetic analyses, a Principal Component Analysis (PCA) was run using the "adegenet" package (Jombart 2008) in R (R Core Team 2017) to check for the presence of other species. The identity of the individuals was additionally confirmed based on allelic size at markers Ld148, Ld158, Ld704, Lo4-24 and Lo454-23 following Mauger et al. (2021). In order to test the independence of each marker, genotypic linkage disequilibrium was calculated for all pairs of markers within and across populations using Genepop 4.7.5 (Rousset 2008). We used 1,000 dememorization, 100 batches and 1,000 iterations per batch for the Markov chain parameters. The presence of null alleles was tested using MICROCHECKER (Van Oosterhout et al. 2004) and genotypes were corrected according to the Van Oosterhout method. Difference between the uncorrected and corrected F_{ST} matrices (pairwise estimates of genetic differentiation, see section below) was checked using a Mantel test available in the "vegan" package (Oksanen et al. 2013). Given the non-independence of the two datasets (corrected and uncorrected), differences in genetic diversity parameters were checked using a Wilcoxon test available in the "stats" R package.

2.5. Population structure

Population structure was first assessed with two multivariate methods: a Principal Coordinate Analysis (PCoA) available in the "ape" package (Paradis & Schliep 2019) and STRUCTURE

v2.3.4 (Pritchard et al. 2000). The PCoA was run as it represents the first step of the distance-based redundancy analysis (db-RDA). STRUCTURE was run with the admixture model without prior population information and 10 independent replicate runs were performed from K = 1 to 20 rather than 32 to reduce computation time. For each replicate, the burn-in was set to 100,000 and the Markov chain Monte Carlo iterations to 500,000 following guidance from Gilbert et al. (2012). The most likely value of K was determined using both Evanno ΔK (Evanno et al. 2005) and log Pr(X|K) methods (Pritchard & Wen 2003) in structureHarvester (Earl & VonHoldt 2012). Based on the recommendations of Janes et al. (2017), the number of genetic clusters was assessed by comparing these two methods. Finally, CLUMPAK (Kopelman et al. 2015) was used to summarize and visualize STRUCTURE outputs. Population structure was additionally investigated with pairwise estimates of F_{ST} (Weir & Cockerham 1984) and confidence intervals were obtained with 95% confidence level and 1,000 resampling procedure using the "hierfstat" package (Goudet 2005). A Wilcoxon test was performed to test the null hypothesis that the average F_{ST} associated with divergent (*i.e.*, populations associated with the highest F_{ST} values) and the rest of the populations did not significantly differ. The same test was used to test the effect of the location (*i.e.*, island or mainland) on F_{ST} values, this test was performed on the continuous dataset (S1 to S24), as no islands were sampled from S25 to S32 (Figure 1 and Table 1).

2.6. Genetic diversity

Single and multilocus estimates of genetic diversity were calculated for each population as the expected heterozygosity (*He*, *sensu* Nei 1978), observed heterozygosity (*Ho*) and the mean number of private alleles ($\overline{Pa}$) using GenAlEx 6.5 (Peakall & Smouse 2006). In addition, standardized allelic richness (*Ar*) was computed using the rarefaction method in "hierfstat". Departure from Hardy Weinberg equilibrium (F_{IS}) was calculated according to the method of Weir & Cockerham (1984) in GENETIX 4.02 (Belkhir et al. 2004) as well as the 1,000 permutations computed to test for their statistical significance. Wilcoxon tests were used to assess the effect of the type (*i.e.*, divergent or not) and the location (island or mainland) on each estimator of genetic diversity and F_{IS}. As previously stated, the effect of the location was performed on the continuous dataset.

2.7. Connectivity model

2.7.1. Hydrodynamic modeling

Flow fields were provided by a 3D regional configuration (MANGA2500) of the MARS3D hydrodynamic model (Petton et al. 2023). The model domain ranges from 41°N to 55°N in latitude, and 18°W to 9°30′E in longitude, encompassing all studied populations from southern Brittany to the Strait of Dover. The domain is resolved horizontally by a regular 2.5 km grid and vertically by 40 sigma levels. The model was forced by meteorological conditions obtained from the ARPEGE and AROME models (Yessad 2015) for the nested zooms with spatial and temporal resolutions of 2.5 km and 1 h, respectively. At the boundaries of the global 3D domain, tidal forcing was provided by a larger 2D model covering the northwest Atlantic, driven by 14 tidal constituents (Lyard et al. 2006).

2.7.2. Lagrangian Modeling

The Lagrangian trajectory of the particles (meiospores or fertile parts of the thallus) was simulated using ICHTHYOP v.3.3.6 (Lett et al. 2008), which employed the hourly 3D flow fields as input data. Particles were released within circles with a radius of 2 km and were allowed to drift for 15 days to account for dispersal by fertile thallus and by meiospores while reducing the duration of the simulations. The computational time step of the Lagrangian model was set to 300 s and the position of the particle was recorded every 20 min. For each simulation, 5,000 particles were released every two hours. This configuration was applied for each location, repeated for eight days per month from June to October (corresponding to *L. digitata*'s highest peak of fertility, Bartsch et al. 2008), using the hydrodynamic outputs of years 2014 and 2015. The eight days were chosen by randomly selecting two days per week in order to account for tidal variation occurring over a month while reducing computational time. A total of 960 dispersal events were hence simulated over two years for each site. Pairwise oceanographic connectivity (P_{ij}) was estimated following Reynes et al. (2021) and is defined as: $P_{ij} = N_{i\text{-}j}/N_i$, with N_i corresponding to the total number of released particles from site i and $N_{i\text{-}j}$ the total number of released particles from i arriving at j within 15 days of dispersal. P_{ij} was then averaged over the full period of the simulation to obtain the mean

connectivity matrix. The level of self-recruitment (P_{ii}) was estimated with the same method as P_{ij} but using a threshold of 48 h to distinguish emitted particles (from the release area) from those returning to the release area after 48 h. A Wilcoxon test was performed to assess the effect of the type (*i.e.,* divergent or not) or the pair of populations (continuous dataset) on the rate of self-recruitment.

2.8. Geographic distance and habitat discontinuity

The bathymetric contour was extracted from a 0.001°-resolution digital terrain model (or DTM, data.shom.fr) using ArcGIS 10. In order to standardize the calculation of pairwise distances between coastal populations around the peninsula, distances were calculated following the 5 m isobath. However, when at least one of the populations was situated on an island, the straight-line distance across the sea was considered. A 0.009º-resolution raster layer representing the distribution of rocky seabed in the English Channel and around Brittany was prepared from the best available substrate information available at Ifremer in May 2019. Information regarding the spatial distribution of bedrock comes from the combination of several sources: (1) maps of coastal habitats produced as part of the Rebent project, with the scales varying from 1/2,000 to 1/10,000; (2) maps of existing habitat produced as part of the MESH project (Bajjouk 2005), with the scales varying from 1/50,000 to 1/10,0000 and (3) from the local extraction of the information on the presence of rock from topo-bathymetric Lidar data (DTM of 5 m resolution) (Gorman et al. 2013, Bajjouk et al. 2015). This layer was subsequently used to compute the continuity of rocky substrata between pairs of sites. Only the rock extents situated above 5 m depth (corresponding to 5 m below the lowest astronomical tide, Figure 1) were considered in this calculation given that *L. digitata* is considered unable to colonize areas below this depth (Robuchon et al. 2014). The proportion of the geographic distance unoccupied by rocky substrata was considered for subsequent analyses.

2.9. Temperature data

Sea-surface temperature (SST) was generated using E.U. Copernicus Marine Service Information, with 0.05°x0.05° resolution (product with DOI 10.48670/moi-00169 and see Merchant et al. 2019 and Good et al. 2020 for product details). To account for the fact that populations are still trying

to catch up the effect of past temperature variations, we considered SST data obtained for a period of 10 years preceding each sampling year (*i.e.*, from 1995 to 2004 for a population sampled in 2005). While the annual mean and range of annual SST were averaged across the period, the minimum (resp. maximum) was chosen as being the minimum (resp. maximum) SST observed across these 10 years as we can imagine that extreme thermal episodes can represent a strong selection.

2.10. Linking environmental variables to genetic structure

Global (resp. partial) db-RDA (Legendre & Anderson 1999) were conducted to investigate the joint (resp. individual) effect of geographic distance, ocean currents, sampling years, SST (minimum, maximum, mean and range) and habitat discontinuity on the total explained genetic variation. The first two axes of the PCoA performed on the F_{ST} matrix were used as the response variables representing the core of the genetic structure in the db-RDA. The analyses were repeated on three datasets to assess *if* and *how* the contribution of each predictor varied according to the sampling scheme. The *overall* dataset corresponded to the whole dataset (*i.e.,* 32 populations), the *regional* dataset accounted for the 29 populations from Brittany (S1 to S29) and the *continuous* dataset solely included the populations that were continuously sampled along the coast (S1 to S24, Figure 1).

Sampling years were taken into account to assess whether variation in sampling year across samples influenced the contemporary genetic differentiation. The environmental explanatory variables accounting for geographic distance and ocean currents were respectively transformed into distance-based Moran's eigenvector maps (dbMEM, Dray et al. 2006) and Asymmetric Eigenvector Maps (AEM, Blanchet et al. 2008b). dbMEM eigenvectors were computed from the matrix of geographic distance with the "adespatial" package using the default settings for truncations, while only retaining positive eigenvalues as we did not expect any negative autocorrelation between sampling positions (Dray et al. 2006). For the construction of AEMs, the oceanographic connectivity matrix was transformed into a nodes-to-edges matrix and the edges were weighted by the probability of dispersal before calculating AEM eigenvectors with the

318 "adespatial" package. Calculations of dbMEM and AEM eigenvectors were iterated for each
319 dataset following the aforementioned method. It is worth noting that the first eigenvectors in both
320 dbMEMs and AEMs (*e.g.*, AEM1, dbMEM1) are associated with broad-scale patterns while the
321 highest (*e.g.*, dbMEM5, AEM25) highlight finer patterns. To test for correlation between dbMEMs
322 and SST variables, a Spearman correlation was measured using the "stats" package.

323 Prior to each global db-RDA, an elastic net regularized regression was performed using the
324 "glmnet" package (Friedman et al. 2010) with the elastic net mixing parameter α fixed at 0.08 in
325 order to decrease the number of explanatory variables (Ogutu et al. 2012). We considered all
326 independent predictors with Variance Inflation Factor (VIF) below 10 to avoid multicollinearity
327 effects using the vif_func function available on walterxie/ComMA. The remaining variables were
328 then selected via a stepwise forward procedure using the ordiR2step function from the "vegan"
329 package. This function selects variables to build the *optimal* model, defined as the model
330 maximizing the adjusted coefficient of determination (R^2_{adj}), while minimizing the *p*-value
331 (Blanchet et al. 2008a). For partial db-RDAs, the variables were directly selected using the
332 ordiR2step function as the number of explanatory variables were already lower than the sample
333 size. Finally, ANOVAs (1,000 permutations) were performed to assess the significance of each
334 model (global and partial db-RDA), axes and retained variables.

335 ## 3. RESULTS

336 ### 3.1. Preliminary analyses

337 The PCA ran on the whole dataset allowed to identify 12 *Laminaria hyperborea* individuals
338 (Figure S1, Table S1), a sister species with overlapping range distribution (Robuchon et al. 2014).
339 These individuals were sampled in S6 (2 ind.), S9 (1 ind.), S21 (3 ind.), S22 (3 ind.), S25 (1 ind.),
340 S28 (1 ind.) and S30 (1 ind.) and were removed from our dataset, giving a total of 896 individuals
341 of *L. digitata*. No significant genotypic linkage disequilibrium was obtained, neither within nor
342 across populations (Table S2). Null alleles were present at locus Ld158 in five populations (S1,
343 S2, S7, S10 and S19, Table S3) and several homozygous genotypes were corrected by adding an
344 allele which was initially absent from the whole dataset (allelic size 246, Table S4). The same

analyses were rerun on the corrected dataset (detection of MLG, F_{ST}, parameters of genetic diversity, db-RDA etc.), which brought us to the decision to keep our original dataset given: (1) the high correlation between genetic diversity parameters (whichever the parameter, *p*-value of the Wilcoxon tests were always higher than 0.6) and F_{ST} matrices (Tables S5 and S6, Mantel statistic based on Pearson's product-moment correlation r = 0.9993), (2) the acquisition of the same db-RDA results, (3) the correlation between the number of alleles and the number of genotypes with missing data (*p*-value = 0.462) suggesting a negligible presence of null alleles and finally (4) the impossibility to rerun multilocus analyses such as STRUCTURE or linkage disequilibrium analyses due to the fact that MICROCHECKER modifies the original sample numbers.

3.2. Population Structure

According to both ΔK and ln Pr(X|K) methods, K = 2 appeared as the optimal number of genetic clusters (Figure S2). The barplot for K = 2 illustrated a general North-South differentiation, with southern Brittany (S1-S4, referred to as "SB" hereafter) and Saint-Malo Bay (S26-S29, referred to as "SMB" hereafter) being particularly well separated (Figure 2A). ΔK method suggested K = 3 to be the next optimal value, followed by K = 12, while the ln Pr(X|K) method first indicated K = 12 and then K = 3 (Figure S2). The barplot for K = 3 separated SB in another cluster (Figure 2B), and the one for K = 12 additionally separated southwest Brittany (S5-S9), S21 (Locquirec), S25 (Roche-Douvres), SMB, Normandy (S30-S31) and S32 (Wissant), while western and northern populations (S10-S20, S22-S24) remained highly admixed (Figure 2C). From these results, eight major genetic groups can be defined: SB, southwest Brittany (S5-S9), S21, populations from western and northern Brittany (S10-S20, S22-S24), S25, SMB, Normandy and S32 (Figure 3). Among these genetic groups, populations from SB, S21, SMB and S32 were associated with significantly higher mean F_{ST} values (Table 2, and Table S5 for pairwise F_{ST} values and their significance; *p*-value < 0.0001) and will be referred to as *divergent* populations from here onwards. The high mean F_{ST} obtained for S32 can be interpreted from allele frequencies spectra, in particular at loci Ld148, Ld371, Lo454-17 and Lo454-28 (Figure S3). However, allelic spectra were less informative for the remaining divergent populations. STRUCTURE results suggested that island

populations are generally well admixed with coastline populations with the exception of S25 (Figure 2C). This result is supported by the fact that the average values of F_{ST} did not significantly differ between coastline and island populations (p-value = 0.379).

3.3. Genetic diversity

Estimates of genetic diversity averaged over the 11 markers are provided in Table 3. The lowest value was always associated to S32 and the highest to populations at the western tip (S8-S14). Variation in genetic diversity across populations was the highest for *Ar*, with values ranging from 2.542 (S32) to 6.151 (S12, Figure 3). Values of F_{IS} showed a significant deficit of heterozygotes for several populations in the raw dataset. The correction for null alleles did not significantly change the values (F_{IS} = -0.04; 0.02; 0.016; 0.068 and 0.067 after correction for respectively S1, S2, S7, S10 and S19. Wilcoxon test, p-value = 0.421 when only accounting for the five populations) as well as the significance of the departure from Hardy-Weinberg (HW) equilibrium, except for S7 for which the F_{IS} was not significantly different from 0 after correction. One multilocus genotype shared by two individuals was detected in S4 and S28 but was not correlated with any significant deviation from HW equilibrium (Table 3).

The 10 divergent populations were associated with the lowest level of genetic diversity (p-value < 0.001 for *He*, *Ho* and *Ar*, see Figure 3) although the same tendency was not observed for $\overline{Pa}$ (p-value: 0.283). These populations also appeared to have significantly lower F_{IS} values compared to the rest of the populations (p-value = 0.023). In contrast, while genetic diversity estimates were always higher in coastal than island populations, differences were not significant based on Wilcoxon tests (p-value for *He*: 0.347, *Ho*: 0.263, *Ar*: 0.174 and $\overline{Pa}$: 0.165). Similarly, higher F_{IS} values were observed in islands but the difference was, again, not significant (p-value: 0.905).

3.4. Habitat discontinuity

The proportion of habitat discontinuity shown in Table S7 suggested a patchy pattern with several populations appearing particularly isolated. As illustrated by Figure 1, island populations appeared naturally isolated by the absence of continuous favorable substrate (*i.e.*, rocky substrata above 5

399 m depth) connecting them to the nearest mainland or island populations thus revealing high
400 fragmentation. At the same time, the expanse of rocky habitat appeared continuous along northern
401 Brittany (S15-S29) as shown by the small proportion of geographic distance which was
402 unoccupied by rocky substrata. The increase in habitat discontinuity between southern (< S11) and
403 northern populations (> S11) was mainly driven by the topography of the Rade of Brest and its
404 lack of rocky substrata at the 5 m isobath, and even above, as suggested by our dataset on rocky
405 substrata.

406 3.5. Oceanographic connectivity

407 Connectivity probabilities resulting from Lagrangian simulations are shown in Figure 4 and Table
408 S8. In most cases, the highest probabilities of connectivity were associated with neighboring
409 populations. Contrastingly, groups of populations such as SB, SMB and Normandy appeared
410 highly connected to each other, but isolated from other populations (Figure 4). The probability of
411 connectivity of S32 with any other population was null, highlighting its strong isolation. In the
412 case of S21, while a particle released from this population attained neighboring populations, this
413 was not true for the other way around, as suggested by the low probabilities that particles released
414 from neighboring populations recruited in S21. The difference between divergent and non-
415 divergent populations was noticeable when comparing the number of connectivity links, defined
416 as the mean number of populations with which the probability of connectivity is different from 0
417 (Table S8). Indeed, spores released from divergent populations reached on average 5.2 populations
418 compared to 7.9 for non-divergent populations. Similarly, spores recruiting in divergent
419 populations originated on average from 4.9 populations, compared to 9.1 for non-divergent ones.
420 The difference in connectivity was less pronounced between island and coastal populations: spores
421 released from islands reached on average 8.5 populations, compared to 6.6 for coastal populations;
422 and spores recruiting in islands originated from an average of 9.2 populations, compared to 6.5 for
423 coastal populations.

424 In terms of directionality, dispersal appeared to have a north-western direction in the south of the
425 Peninsula (S1-S7) and a north-eastern direction when considering north-western and northern

populations (S10-S25, Figure 4). For instance, a spore released from S10 reached S11 to S14 with a higher probability than in the opposite direction (Figure 4, Table S8). The pattern became less clear from SMB. However, as previously stated, these populations tended to be highly connected within each genetic group (SMB, Normandy) but not with populations beyond them, making directionality analyses less relevant.

Finally, self-recruitment probability varied from 0.005 (S8) to 0.476 (S25, Table S8). The probability did not significantly differ between island and coastline populations (0.211 and 0.189, respectively, *p*-value = 0.077), nor between divergent and non-divergent populations (0.255 and 0.169, respectively, *p*-value = 0.64).

3.6. Hierarchical effects of environmental factors on genetic structure

Whichever the geographical scale, habitat discontinuity and sampling years were not retained in the global nor partial db-RDA (Table 4). Therefore, for the sake of parsimony, these two variables will not be mentioned in the following results.

3.6.1. Overall dataset

The model and the two first axes associated with the global db-RDA were significant (*p*-value < 0.001) with an adjusted coefficient of determination (R^2_{adj}) of 0.604 (Table 4). Five variables were selected by the ordiR2step function which were related to geographic distance (dbMEM1, 3 and 5) and oceanographic connectivity (AEM1 and 3, Table 4, Figure 5B). The first axis, accounting for 71.6% of the variance, showed a clear differentiation between southern and northern Brittany which appeared to be driven by geographic distance (dbMEM1, Figure 5B) and by oceanographic processes to a lesser extent (AEM1 and 3, Figure 5B and S4). The second axis, accounting for 18.1% of the variance and mostly driven by geographic distance (dbMEM3), isolated S32 whilst populations from Normandy remained poorly differentiated (Figure 5B). When partitioning the respective effects of oceanographic connectivity, geographical distance and SST using partial db-RDA, each predictor appeared significant. Geographic distance explained the greatest amount of variance with R^2_{adj} = 0.475, against 0.165 for SST (minimum and mean) and 0.115 for oceanographic connectivity (Table 4).

453 3.6.2. Regional dataset

454 To investigate the relative contribution of each environmental factor at a regional scale,
455 populations S30, S31 and S32 were excluded because of their high geographic isolation (*ca*. 600
456 km from the rest of the populations). The model and the two first axes associated with the global
457 db-RDA were again significant (p-value < 0.001) with $R^2_{adj} = 0.614$ (Table 4). Six variables were
458 retained by the ordiR2step selection process: two accounted for geographic distance (dbMEM2
459 and 3, Table 4) and four for oceanographic connectivity (AEM1, 2, 23 and 25, Table 4). The first
460 axis (84.9% of the variance) was driven by geographic distance (dbMEM2, Figure 5C), while
461 oceanographic processes appeared important for finer genetic structure (Figure S4). The first axis
462 again clearly separated populations according to their latitude and SMB appeared isolated due to
463 geographic distance. The second axis (10.3%) was driven by AEM25 and isolated S21, suggesting
464 the role of oceanographic currents on its genetic isolation (Figure 5C). When partitioning the
465 respective effects of oceanographic connectivity, geographical distance and SST, each predictor
466 appeared significant. With this dataset, oceanographic connectivity explained a slightly higher
467 amount of variance compared to geographic distance ($R^2_{adj} = 0.549$ and 0.485, respectively) while
468 $R^2_{adj} = 0.221$ for SST (mean, Table 4).

469 3.6.3. Continuous dataset

470 The third analysis accounting for the 24 continuously sampled populations (S1-S24) was
471 performed by additionally excluding SMB and S25. At this scale, the highest distance between
472 two neighboring populations is reduced to *ca*. 160 km (between S11 and S12 when following
473 coastline) without any major gap in connectivity (Figure 4). The model and the three first axes
474 were significant (p-value < 0.001 for the model and the first axis, p-value < 0.05 for the remaining
475 two axes) with $R^2_{adj} = 0.777$ (Table 4). Eight variables remained after the two selection processes:
476 seven associated to oceanographic currents (AEM1, 2, 3, 5, 10, 16 and 19) and one to geographic
477 distance (dbMEM3, Table 4, Figure 5D). This first axis was mostly explained by AEM1, denoting
478 a gradual north-wise differentiation (Figure 5D), whilst higher order AEMs mostly revealed the
479 strong density of connectivity links amongst northern (S10-S25) or southern populations (S1-S7,

480 Figure S4). The second axis was mostly driven by AEM5, which again isolated S21. With this
481 dataset, oceanographic connectivity explained a greater amount of variance than geographic
482 distance (R^2_{adj} = 0.794 and 0.513, respectively) denoting the fact that genetic differentiation
483 between populations was widely explained by oceanographic processes, while SST explained
484 21.0% of the variance (maximum SST).
485 Finally, whichever the dataset, SST was never retained in global db-RDAs, which is most likely
486 due to the correlation between some of the SST-related variables and dbMEMs observed
487 whichever the datasets (Table S9).
488 4. DISCUSSION
489 Our study builds on previous microsatellite research (Billot et al. 2003, Valero et al. 2011,
490 Couceiro et al. 2013, Robuchon et al. 2014) to refine our understanding of *Laminaria digitata*'s
491 population structure in the southern edge of its East Atlantic distribution. We specifically aimed at
492 deepening our knowledge of connectivity patterns among the studied populations which comprised
493 22 coastline and 10 on-shelf island populations. To do this, we combined inference and analyses
494 of genetic structure, genetic diversity and dispersal probabilities resulting from Lagrangian
495 simulations. This enabled us to identify divergent populations, defined as those associated with
496 high genetic differentiation and poor diversity, surrounded by highly connected populations
497 associated with high genetic diversity. This pattern is consistent with the ecological and
498 demographic status of *L. digitata* forest which has been described as highly contrasted in the
499 studied area, ranging from a "no declined reported" status in north-western Brittany to a "local
500 decline" status in South Brittany and Saint-Malo Bay (de Bettignies et al. 2021). We additionally
501 compared connectivity patterns between coastal and island populations and found that island
502 populations are generally well connected to other islands or coastal populations. A distance-based
503 redundancy analysis (db-RDA) was applied to disentangle the contribution of various
504 environmental factors which are thought to influence connectivity and thus genetic structure,
505 namely: habitat discontinuity, geographical distance, hydrodynamic processes, sea surface
506 temperature (SST) and sampling year. This analysis was repeated for three datasets corresponding

507 to varying sampling schemes, as we expect the presence of rocky substrata, hydrodynamic features
508 and SST to vary at relatively small spatial scales. Overall, our analyses have shown that the amount
509 of variation explained by seascape features increased as the sampling gap between sampled
510 populations was reduced. Our study therefore shows how the conclusions heavily depend on the
511 presence and extent of sampling gaps. Given that seascape genetics tools are nowadays being more
512 and more used, we call for greater attention in the conclusions that are drawn.

513 Analyses of population structure have shown a discrepancy between southern and northern
514 Brittany, which can be related to oceanic currents according to the db-RDA run on the dataset with
515 continuously distributed populations. This discrepancy is in line with the fact that this region
516 corresponds to an oceanographic boundary: while the main ocean current in the southern coast of
517 Brittany corresponds to the shelf residual current which has a northwest-ward direction, northern
518 Brittany is dominated by the English Channel residual circulation which has a northeast-ward
519 direction (Pingree & Le Cann 1989). This genetic divergence was also reported for other species
520 (Roman & Palumbi 2004, Jolly et al. 2006, Nunes et al. 2021) and could also correspond to the
521 limit between the northern European Sea and the Lusitanian biogeographical provinces which was
522 pointed out to explain the biogeographic breaks observed in various marine taxa (Spalding et al.
523 2007). The directionality observed in the Lagrangian simulations is consistent with the direction
524 of these two major currents, albeit the variation in directionality due to tides and winds (Ayata et
525 al. 2010).

526 Previous results on *L. digitata* have shown significant population differentiation from 1 to
527 10 km (Billot et al. 2003, Valero et al. 2011, Robuchon et al. 2014), a fine-scale genetic structure
528 supported by the commonly reported short dispersal distance in kelps (Dayton 1985, Norton 1992).
529 Contrastingly, our results suggest that genetic differentiation was not significant between several
530 pairs of populations separated by more than 50 km, particularly for populations located in western
531 and north-western Brittany. Low genetic differentiation at large geographic distances was
532 particularly clear for island populations which were separated by more than 100 km from the coast
533 and despite the absence of continuous favorable substrate (*i.e.*, rocky substrata above 5 m depth)

connecting them to the nearest mainland or island populations. In fact, the number of connectivity links (defined as the mean number of populations with which the probability of connectivity is non null), as well as values of genetic differentiation and of genetic diversity revealed that islands are generally well connected. Nonetheless, this conclusion might be affected by species' means of dispersal and should not be taken as a general rule. In addition, we have only considered on-shelf coastal populations which were connected to the mainland at the Last Glacial Maximum when the sea level was 100 to 120 m below present (Frenzel et al. 1992, Lambeck 1997). These islands therefore share the same evolutionary history as populations found along the coastline, and this historical pattern is expected to influence the observed low genetic differentiation of island populations.

In contrast to the low genetic differentiation observed for island populations, our analyses have revealed genetically divergent populations, associated with high genetic differentiation and significantly lower values of genetic diversity. Amongst these divergent populations, the ones from southern Brittany and Saint-Malo Bay appeared to be particularly differentiated. Results from Lagrangian simulations have shown that populations within these two genetic clusters are highly connected but largely unrelated to other populations. Nonetheless, results from db-RDA revealed that Saint-Malo Bay was genetically isolated due to geographic distance rather than by the occurrence of tidal gyres, as previously suggested by Billot et al. (2003) and Robuchon et al. (2014). However, geographic distance might appear as the causal factor for the divergence of Saint-Malo Bay due to gaps in the sampling. Indeed, by repeating the db-RDA on three datasets, we have demonstrated how sampling schemes can greatly influence the conclusions that can be drawn. In particular, we have shown that as the extent of the sampling gaps decreased, the relative importance of ocean currents (mainly in relation to geographic distance) increased. Therefore, our dataset does not allow us to properly infer the origin of the genetic isolation of Saint-Malo Bay.

In addition to South Brittany and Saint-Malo Bay, two other divergent populations were identified: Locquirec, which also appeared highly differentiated from surrounding populations at small spatial scale (< 20 km), and the geographically isolated population of Wissant. All of these

561 divergent populations (populations from South Brittany, Saint-Malo Bay, Locquirec and Wissant)
562 were associated with lower genetic diversity, with Wissant being particularly impoverished.
563 Unlike what has been previously suggested by Billot et al. (2003), the results of the db-RDA as
564 well as the ones from Lagrangian simulations suggest that Locquirec is isolated due to oceanic
565 currents. This result is supported by the description of eddies at the entrance of Lannion Bay and
566 a slow residual current within the Bay (Beslier et al. 1980, Garreau 1993). This confirms that ocean
567 currents not only affect long-distance dispersal (*e.g.*, between islands and coastline) but also have
568 localized effects as reported for *L. digitata* in Strangford Narrows (Brennan et al. 2014) and for
569 other species of seaweed characterized by low dispersal abilities (Buonomo et al. 2017, Reynes et
570 al. 2021). Nonetheless, habitat appeared highly discontinuous between Locquirec and its
571 surrounding populations (> 90% of the total distance is devoid of rocky substrata above 5 m depth),
572 which could intensify the genetic isolation of this population. As opposed to Locquirec, geographic
573 distance appears as the main cause for the isolation of Wissant. In this case, a finer sampling
574 scheme along the French coast might not change the results given the absence of nearby
575 populations (Araújo et al. 2016). The low genetic diversity measured on neutral markers reflects a
576 low effective population size and thus higher strength of genetic drift (compared to selection),
577 which ultimately leads to an increase in the probability of going extinct. Careful attention and
578 appropriate conservation measures should therefore be taken in order to prevent this end.

579 The stepwise variable selection procedure applied prior to each global db-RDA has never
580 selected variables associated with sampling year, SST or habitat discontinuity. Although
581 parameters associated to SST were significant in partial db-RDA, habitat discontinuity was never
582 significant despite the findings on other kelp species (Alberto et al. 2010, 2011, Selkoe et al. 2010,
583 Johansson et al. 2015). This discrepancy could stem from the fact that our rock layer was built by
584 combining various data with different precisions, or from the fact that the calculation of habitat
585 discontinuity was constrained by the 5 m bathymetric contour. Another argument is that Alberto
586 et al. (2010, 2011) and Selkoe et al. (2010) have measured habitat continuity by looking at kelp
587 coverage rather than proportion of rocky substrata *per se*. Yet, evidence from other kelp species

suggests that sporophyte recruitment largely depends on meiospore density ensuring sperm-egg encountering (Reed 1990). By considering kelp coverage rather than rocky substrata, Alberto et al. (2010, 2011) and Selkoe et al. (2010) might have incorporated the effect of meiospores dilution into habitat discontinuity, which was not our case. Nonetheless, the use of other methods (e.g., resistance matrix, Wilcox et al. 2023) could have led to other conclusions.

The fact that SST variables were never retained in global db-RDA could stem from the limitation to the use of dbMEMs which may underestimate the importance of other environmental variables that show some correlations with one of these Moran's eigenvector decomposition (Dalongeville et al. 2018). To overcome this limitation, one could consider hourly temperature data (*e.g.*, from *in situ* dataloggers) which, in addition to its relevance for intertidal species, could decrease the correlation with dbMEMs. Despite these results, partial db-RDA accounting for SST were significant whichever the datasets, therefore pointing out its relevance in explaining genetic structure. This could be particularly true for this kelp species as sporulation has been shown to be severely impacted at temperatures above 17°C (Bartsch et al. 2013), yet SST in southern Brittany reaches 21°C in summer (Gallon et al. 2014). Although mechanisms linked to sporulation could be adapted to higher temperature, Oppliger et al. (2014) have shown that the mean number of released meiospores is significantly lower in Quiberon (corresponding to S4) compared to a population in northern Brittany. Yet a decreased amount of released meiospores should lead to a decreased connectivity and thus higher genetic differentiation. This underlines the fact that SST could have various consequences on life history traits in *L. digitata* which should be apparent on data obtained using neutral markers through the phenomenon of isolation by adaptation (Nosil et al. 2009, Schoville et al. 2012). Similarly, the sharp genetic break observed between southwestern populations (S5-S9) and southern Brittany could have also been attributed to the difference in SST between these two regions.

Conclusion

Our study revealed a mosaic of connectivity patterns with well-connected populations surrounded by populations that appeared less connected and less diverse, with the population of Wissant being particularly impoverished. This pattern is consistent with the ecological and demographic status of *Laminaria digitata* forest which has been described as highly contrasted in the studied area. Various db-RDA were conducted to deepen our understanding of the observed genetic variation. Unlike previous studies carried out on *L. digitata* as well as on other kelp species, our results indicated a limited effect of habitat fragmentation compared to ocean currents and geographic distance. Moreover, the relative effect of these two latter environmental variables varied according to sampling schemes: while geographic distance was particularly relevant in our overall dataset, which included sampling gaps of more than 600 km, oceanographic processes appeared as the main drivers at finer spatial resolution.

Acknowledgements

We thank Eric Thiébaut, Thierry Comtet, Jean-François Arnaud and Ophélie Ronce for helpful discussions and comments. The OSU Pythéas Institute (Marseille) is thanked for the use of the high-performance computing (HPC) cluster. We are also grateful to the Biogenouest genomics core facility (Genomer Plateforme génomique at the Biological Station of Roscoff in particular Gwenn Tanguy) for their technical support. We additionally warmly thank several phycologists, the Marine Observation Department and the diving team of the Biological Station of Roscoff for sampling, and François Gevaert for his valuable insights regarding the rare occurrence of *L. digitata* in the strait of Dover. LF was funded by the EU project MARFOR Biodiversa/004/2015, Region Bretagne (ARED 2017 REEALG) and the NOMIS-ISTA Fellowship Program. JA is funded by Portuguese national funds through projects UIDB/04326/2020, UIDP/04326/2020, LA/P/0101/2020, PTDC/BIA-CBI/6515/2020 and the Individual Call to Scientific Employment Stimulus 2022.00861.CEECIND.

Competing interests

The authors declare no competing interests.

References

Aeschbacher S, Selby JP, Willis JH, Coop G (2017) Population-genomic inference of the strength and timing of selection against gene flow. Proc Natl Acad Sci 114:7061–7066.

Alberto F, Raimondi PT, Reed DC, Coelho NC, Leblois R, Whitmer A, Serrão EA (2010) Habitat continuity and geographic distance predict population genetic differentiation in giant kelp. Ecology 91:49–56.

Alberto F, Raimondi PT, Reed DC, Watson JR, Siegel DA, Mitarai S, Coelho N, Serrão EA (2011) Isolation by oceanographic distance explains genetic structure for *Macrocystis pyrifera* in the Santa Barbara Channel. Mol Ecol 20:2543–2554.

Arafeh-Dalmau N, Montaño-Moctezuma G, Martínez JA, Beas-Luna R, Schoeman DS, Torres-Moye G (2019) Extreme marine heatwaves alter kelp forest community near its equatorward distribution limit. Front Mar Sci 6.

Araújo RM, Assis J, Aguillar R, Airoldi L, Bárbara I, Bartsch I, Bekkby T, Christie H, Davoult D, Derrien-Courtel S, Fernandez C, Fredriksen S, Gevaert F, Gundersen H, Le Gal A, Lévêque L, Mieszkowska N, Norderhaug KM, Oliveira P, Puente A, Rico JM, Rinde E, Schubert H, Strain EM, Valero M, Viard F, Sousa-Pinto I (2016) Status, trends and drivers of kelp forests in Europe: An expert assessment. Biodivers Conserv 25:1319–1348.

Ayata SD, Lazure P, Thiébaut É (2010) How does the connectivity between populations mediate range limits of marine invertebrates? A case study of larval dispersal between the Bay of Biscay and the English Channel (North-East Atlantic). Prog Oceanogr 87:18–36.

Bajjouk T (2005) Traitement et structuration des données en zones côtières. Projet MESH. Contrat Ifremer-Capgemini N° 04/2 210 934. 29p.

Bajjouk T, Rochette S, Laurans M, Ehrhold A, Hamdi A, Le Niliot P (2015) Multi-approach mapping to help spatial planning and management of the kelp species *Laminaria digitata* and *Laminaria hyperborea*: Case study of the Molène Archipelago, Brittany. J Sea Res 100:2–21.

Bartsch I, Vogt J, Pehlke C, Hanelt D (2013) Prevailing sea surface temperatures inhibit summer reproduction of the kelp *Laminaria digitata* at Helgoland (North Sea). J Phycol 49:1061–1073.

Bartsch I, Wiencke C, Bischof K, Buchholz CM, Buck BH, Eggert A, Feuerpfeil P, Hanelt D, Jacobsen S, Karez R, Karsten U, Molis M, Roleda MY, Schubert H, Schumann R, Valentin K, Weinberger F, Wiese J (2008) The genus *Laminaria* sensu lato: Recent insights and developments. Eur J Phycol 43:1–86.

Belkhir K, Borsa P, Chikhi L, Raufaste N, Bonhomme F (2004) GENETIX 4.05, logiciel sous Windows pour la génétique des populations. Laboratoire Génome, Populations, Interactions, CNRS UMR 5000, Université de Montpellier II, Montpellier.

Bell PR (2008) Connectivity between island Marine Protected Areas and the mainland. Biol Conserv 141:2807–2820.

Benestan L, Loiseau N, Guérin P, Pérez-Ruzafa A, Forcada A, Arcas E, Lenfant P, Mallol S, Goñi R, Velez L, Mouillot D, Puebla O, Manel S (2023) Contrasting influence of seascape, space and marine reserves on genomic variation in multiple species. Ecography 2023.

Benestan L, Quinn BK, Maaroufi H, Laporte M, Clark FK, Greenwood SJ, Rochette R, Bernatchez L (2016) Seascape genomics provides evidence for thermal adaptation and current-mediated population structure in American lobster (*Homarus americanus*). Mol Ecol 25:5073–5092.

Benestan LM, Rougemont Q, Senay C, Normandeau E, Parent E, Rideout R, Bernatchez L, Lambert Y, Audet C, Parent GJ (2021) Population genomics and history of speciation reveal fishery management gaps in two related redfish species (*Sebastes mentella* and *Sebastes fasciatus*). Evol Appl 14:588–606.

Beslier A, Birrien JL, Cabioch L, Larsonneur C, Borgne L (1980) La pollution des Baies de Morlaix et de Lannion par les hydrocarbures de l' "Amoco Cadiz": Répartition sur les fonds et évolution. Helgoländer Meeresunters 33:209–224.

de Bettignies T, Hébert C, Assis J, Bartsch I, Bekkby T, Christie H, Dahl K, Derrien-Courtel S,

Edwards H, Filbee-Dexter K, Franco J, Gillham K, Harrald M, Hennicke J, Hernández S, Le Gall L, Martinez B, Mieszkowska N, Moore P, Moy F, Mueller M, Norderhaug KM, Parry M, Ramsay K, Robuchon M, Russel T, Serrão E, Smale D, Steen H, Street M, Tempera F, Valero M, Werner T, La Rivière M (2021) Case Report for kelp forests habitat. OSPAR 787/2021.

Billot C, Engel CR, Rousvoal S, Kloareg B, Valero M (2003) Current patterns, habitat discontinuities and population genetic structure: The case of the kelp *Laminaria digitata* in the English Channel. Mar Ecol Prog Ser 253:111–121.

Billot C, Rousvoal S, Estoup A, Epplen JT, Saumitou-Laprade P, Valero M, Kloareg B (1998) Isolation and characterization of microsatellite markers in the nuclear genome of the brown alga *Laminaria digitata* (Phaeophyceae). Mol Ecol 7:1778–1780.

Blanchet FG, Legendre P, Borcard D (2008a) Forward selection of explanatory variables. Ecology 89:2623–2632.

Blanchet FG, Legendre P, Borcard D (2008b) Modelling directional spatial processes in ecological data. Ecol Model 215:325–336.

Blauw A, Eleveld M, Prins T, Zijl F, Groenenboom J (2019) Coherence in assessment framework of chlorophyll a and nutrients as part of the EU project 'Joint monitoring programme of the eutrophication of the North Sea with satellite data'.

Boussarie G, Momigliano P, Robbins WD, Bonnin L, Cornu J, Fauvelot C, Kiszka JJ, Manel S, Mouillot D, Vigliola L (2022) Identifying barriers to gene flow and hierarchical conservation units from seascape genomics: a modelling framework applied to a marine predator. Ecography 2022.

Brennan G, Kregting L, Beatty GE, Cole C, Elsäßer B, Savidge G, Provan J (2014) Understanding macroalgal dispersal in a complex hydrodynamic environment: A combined population genetic and physical modelling approach. J R Soc Interface 11:1–12.

Bridle JR, Gavaz S, Kennington WJ (2009) Testing limits to adaptation along altitudinal gradients in rainforest Drosophila. Proc R Soc B Biol Sci 276:1507–1515.

Buonomo R, Assis J, Fernandes F, Engelen AH, Airoldi L, Serrão EA (2017) Habitat continuity and stepping-stone oceanographic distances explain population genetic connectivity of the brown alga *Cystoseira amentacea*. Mol Ecol 26:766–780.

Capblancq T, Forester BR (2021) Redundancy analysis: A Swiss Army Knife for landscape genomics. Methods Ecol Evol 12:2298–2309.

Cavanaugh KC, Reed DC, Bell TW, Castorani MCN, Beas-Luna R (2019) Spatial variability in the resistance and resilience of giant kelp in Southern and Baja California to a multiyear heatwave. Front Mar Sci 6.

Coelho NC, Serrão EA, Alberto F (2014) Characterization of fifteen microsatellite markers for the kelp Laminaria ochroleuca and cross species amplification within the genus. Conserv Genet Resour 6:949–950.

Coleman MA, Minne AJP, Vranken S, Wernberg T (2020) Genetic tropicalisation following a marine heatwave. Sci Rep 10:1–11.

Coleman MA, Veenhof RJ (2021) Reproductive versatility of kelps in changing oceans. J Phycol 57:708–710.

Couceiro L, Robuchon M, Destombe C, Valero M (2013) Management and conservation of the kelp species *Laminaria digitata*: Using genetic tools to explore the potential exporting role of the MPA "Parc naturel marin d'Iroise." Aquat Living Resour 26:197–205.

D'Aloia CC, Bogdanowicz SM, Harrison RG, Buston PM (2014) Seascape continuity plays an important role in determining patterns of spatial genetic structure in a coral reef fish. Mol Ecol 23:2902–2913.

Dalongeville A, Andrello M, Mouillot D, Lobreaux S, Fortin M-J, Lasram F, Belmaker J, Rocklin D, Manel S (2018) Geographic isolation and larval dispersal shape seascape genetic patterns differently according to spatial scale. Evol Appl 11:1437–1447.

Dawson MN (2016) Island and island-like marine environments. Glob Ecol Biogeogr 25:831–846.

750 Dayton PK (1985) Ecology of kelp communities. Annu Rev Ecol Syst Vol 16:215–245.
751 Dray S, Legendre P, Peres-Neto PR (2006) Spatial modelling: a comprehensive framework for
752 principal coordinate analysis of neighbour matrices (PCNM). Ecol Model 196:483–493.
753 DuBois K, Pollard KN, Kauffman BJ, Williams SL, Stachowicz JJ (2022) Local adaptation in a
754 marine foundation species: Implications for resilience to future global change. Glob
755 Change Biol 28:2596–2610.
756 Durrant H, Barrett N, Edgar G, Coleman M, Burridge C (2018) Seascape habitat patchiness and
757 hydrodynamics explain genetic structuring of kelp populations. Mar Ecol Prog Ser 587:81–
758 92.
759 Earl DA, VonHoldt BM (2012) STRUCTURE HARVESTER: a website and program for
760 visualizing STRUCTURE output and implementing the Evanno method. Conserv Genet
761 Resour 4:359–361.
762 Engel CR, Destombe C, Valero M (2004) Mating system and gene flow in the red seaweed
763 *Gracilaria gracilis*: Effect of haploid-diploid life history and intertidal rocky shore
764 landscape on fine-scale genetic structure. Heredity 92:289–298.
765 Evanno G, Regnaut S, Goudet J (2005) Detecting the number of clusters of individuals using the
766 software STRUCTURE: A simulation study. Mol Ecol 14:2611–2620.
767 Fernández C (2011) The retreat of large brown seaweeds on the north coast of Spain: the case of
768 *Saccorhiza polyschides*. Eur J Phycol 46:352–360.
769 Filbee-Dexter K, Feehan C, Scheibling R (2016) Large-scale degradation of a kelp ecosystem in
770 an ocean warming hotspot. Mar Ecol Prog Ser 543:141–152.
771 Filbee-Dexter K, Wernberg T, Grace SP, Thormar J, Fredriksen S, Narvaez CN, Feehan CJ,
772 Norderhaug KM (2020) Marine heatwaves and the collapse of marginal North Atlantic kelp
773 forests. Sci Rep 10:1–11.
774 Frenzel B, Beug H-J, Brunnacker K, Busche D, Frankenberg P, Fritz P, Geyh MA, Hagedorn H,
775 Hövermann J, Kessler A, Königswald W v., Krumsiek K, Lauer W, Mensching H, Moser
776 H, Münnich K-O, Sonntag Chr, Vinken R (1992) Climates during the Last Glacial
777 Maximum. In: *Atlas of paleoclimates and paleoenvironments of the Northern Hemisphere*.
778 Frenzel B, Pécsi M, Velichko AA (eds) Geographical Research Institute, Hungarian
779 Academy of Sciences, Budapest; Gustav Fischer Verlag, Stuttgart; Jena; New York
780 Friedman J, Hastie T, Tibshirani R (2010) Regularization paths for generalized linear models via
781 coordinate descent. J Stat Softw 33:1–20.
782 Gaggiotti OE, Bekkevold D, Jørgensen HBH, Foll M, Carvalho GR, Andre C, Ruzzante DE
783 (2009) Disentangling the effects of evolutionary, demographic and environmental factors
784 influencing genetic structure of natural populations: Atlantic herring as a case study.
785 Evolution 63:2939–2951.
786 Gallon RK, Robuchon M, Leroy B, Le Gall L, Valero M, Feunteun E (2014) Twenty years of
787 observed and predicted changes in subtidal red seaweed assemblages along a
788 biogeographical transition zone: Inferring potential causes from environmental data. J
789 Biogeogr 41:2293–2306.
790 Garineaud C (2021) Appréhender et s'adapter. Rev D'ethnoécologie:0–25.
791 Garreau P (1993) Hydrodynamics of the North Brittany coast: a synoptic study. Oceanol Acta
792 16:469–477.
793 Gaylord B, Gaines SD (2000) Temperature or transport? Range limits in marine species mediated
794 solely by flow. Am Nat 155:769–789.
795 Gilbert KJ, Andrew RL, Bock DG, Franklin MT, Kane NC, Moore JS, Moyers BT, Renaut S,
796 Rennison DJ, Veen T, Vines TH (2012) Recommendations for utilizing and reporting
797 population genetic analyses: The reproducibility of genetic clustering using the program
798 structure. Mol Ecol 21:4925–4930.
799 Gilg MR, Hilbish TJ (2003) The geography of marine larval dispersal: coupling genetics with
800 fine-scale physical oceanography. Ecology 84:2989–2998.
801 Good S, Fiedler E, Mao C, Martin MJ, Maycock A, Reid R, Roberts-Jones J, Searle T, Waters J,
802 While J, Worsfold M (2020) The current configuration of the OSTIA system for

operational production of foundation sea surface temperature and ice concentration analyses. Remote Sens 12:720.
Gorman D, Bajjouk T, Populus J, Vasquez M, Ehrhold A (2013) Modeling kelp forest distribution and biomass along temperate rocky coastlines. Mar Biol 160:309–325.
Goudet J (2005) HIERFSTAT, a package for R to compute and test hierarchical F-statistics. Mol Ecol Notes 5:184–186.
Graves TA, Beier P, Royle JA (2013) Current approaches using genetic distances produce poor estimates of landscape resistance to interindividual dispersal. Mol Ecol 22:3888–3903.
Grummer JA, Beheregaray LB, Bernatchez L, Hand BK, Luikart G, Narum SR, Taylor EB (2019) Aquatic Landscape Genomics and Environmental Effects on Genetic Variation. Trends Ecol Evol 34:641–654.
Guzinski J, Ruggeri P, Ballenghien M, Mauger S, Jacquemin B, Jollivet C, Coudret J, Jaugeon L, Destombe C, Valero M (2020) Seascape genomics of the sugar kelp *Saccharina latissima* along the North Eastern Atlantic latitudinal gradient. Genes 11:1503.
Hickey AJR, Lavery SD, Hannan DA, Baker CS, Clements KD (2009) New Zealand triplefin fishes (family Tripterygiidae): contrasting population structure and mtDNA diversity within a marine species flock. Mol Ecol 18:680–696.
Hu ZM, Zhong KL, Weinberger F, Duan DL, Draisma SGA, Serrão EA (2020) Linking ecology to genetics to better understand adaptation and evolution: A review in marine macrophytes. Front Mar Sci 7:1–12.
Janes JK, Miller JM, Dupuis JR, Malenfant RM, Gorrell JC, Cullingham CI, Andrew RL (2017) The K = 2 conundrum. Mol Ecol 26:3594–3602.
Jayathilake DRM, Costello MJ (2020) A modelled global distribution of the kelp biome. Biol Conserv 252:1–10.
Johansson ML, Alberto F, Reed DC, Raimondi PT, Coelho NC, Young MA, Drake PT, Edwards CA, Cavanaugh K, Assis J, Ladah LB, Bell TW, Coyer JA, Siegel DA, Serrão EA (2015) Seascape drivers of *Macrocystis pyrifera* population genetic structure in the northeast Pacific. Mol Ecol 24:4866–4885.
Jolly MT, Viard F, Gentil F, Thiébaut E, Jollivet D (2006) Comparative phylogeography of two coastal polychaete tubeworms in the Northeast Atlantic supports shared history and vicariant events. Mol Ecol 15:1841–1855.
Jombart T (2008) Adegenet: a R package for the multivariate analysis of genetic markers. Bioinformatics 24:1403–1405.
Jombart T, Dray S, Dufour AB (2009) Finding essential scales of spatial variation in ecological data: A multivariate approach. Ecography 32:161–168.
Kain JM (1979) A view of the genus *Laminaria*. Oceanogr Mar Biol Annu Rev 17:101–161.
Klingbeil WH, Montecinos GJ, Alberto F (2022) Giant kelp genetic monitoring before and after disturbance reveals stable genetic diversity in Southern California. Front Mar Sci 9:1–16.
Kopelman NM, Mayzel J, Jakobsson M, Rosenberg NA, Mayrose I (2015) Clumpak: a program for identifying clustering modes and packaging population structure inferences across K. Mol Ecol Resour 15:1179–1191.
Krueger-Hadfield SA, Roze D, Mauger S, Valero M (2013) Intergametophytic selfing and microgeographic genetic structure shape populations of the intertidal red seaweed *Chondrus crispus*. Mol Ecol 22:3242–3260.
Lambeck K (1997) Sea-level change along the French Atlantic and Channel coasts since the time of the Last Glacial Maximum. Palaeogeogr Palaeoclimatol Palaeoecol 129:1–22.
Legendre L, Demers S (1984) Towards Dynamic Biological Oceanography and Limnology. Can J Fish Aquat Sci 41:2–19.
Legendre P, Anderson MJ (1999) Distance-based redundancy analysis: Testing multispecies responses in multifactorial ecological experiments. Ecol Monogr 69:1–24.
Lett C, Verley P, Mullon C, Parada C, Brochier T, Penven P, Blanke B (2008) A Lagrangian tool for modelling ichthyoplankton dynamics. Environ Model Softw 23:1210–1214.
Liesner D, Fouqueau L, Valero M, Roleda MY, Pearson GA, Bischof K, Valentin K, Bartsch I

(2020) Heat stress responses and population genetics of the kelp *Laminaria digitata* (Phaeophyceae) across latitudes reveal differentiation among North Atlantic populations. Ecol Evol:1–34.
Lüning K (1990) Seaweeds: Their Environment, biogeography, and ecophysiology. Wiley & Sons, New York, USA.
Lyard F, Lefevre F, Letellier T, Francis O (2006) Modelling the global ocean tides: modern insights from FES2004. Ocean Dyn 56:394–415.
Lynch M, Lande R (1993) Evolution and extinction in response to environmental change. In: *Biotic interactions and global change*. Kareiva PM, Kingsolver JG, Huey RB (eds) Sinauer Associates: Sunderland, MA, p 234–250
Manel S, Loiseau N, Puebla O (2019) Long-distance marine connectivity: Poorly understood but potentially important. Trends Ecol Evol 34:688–689.
Martins NT, Macagnan LB, Cassano V, Gurgel CFD (2022) Brazilian marine phylogeography: A literature synthesis and analysis of barriers. Mol Ecol 31:5423–5439.
Mauger S, Couceiro L, Valero M (2012) A simple and cost-effective method to synthesize an internal size standard amenable to use with a 5-dye system. Prime Res Biotechnol 2:2315–5299.
Mauger S, Fouqueau L, Avia K, Reynes L, Serrao EA, Neiva J, Valero M (2021) Development of tools to rapidly identify cryptic species and characterize their genetic diversity in different European kelp species. J Appl Phycol 33:4169–4186.
Merchant CJ, Embury O, Bulgin CE, Block T, Corlett GK, Fiedler E, Good SA, Mittaz J, Rayner NA, Berry D, Eastwood S, Taylor M, Tsushima Y, Waterfall A, Wilson R, Donlon C (2019) Satellite-based time-series of sea-surface temperature since 1981 for climate applications. Sci Data 6:223.
Mitarai S, Siegel DA, Watson JR, Dong C, McWilliams JC (2009) Quantifying connectivity in the coastal ocean with application to the Southern California Bight. J Geophys Res 114:C10026.
Nadeau CP, Urban MC (2019) Eco-evolution on the edge during climate change. Ecography 42:1280–1297.
Nei M (1978) Estimation of average heterozygosity and genetic distance from a small number of individuals. Genetics 89:583–590.
Nicolle A, Moitié R, Ogor J, Dumas F, Foveau A, Foucher E, Thiébaut E (2017) Modelling larval dispersal of *Pecten maximus* in the English Channel: A tool for the spatial management of the stocks. ICES J Mar Sci 74:1812–1825.
Norton TA (1992) Dispersal by macroalgae. Br Phycol J 27:293–301.
Nosil P, Funk DJ, Ortiz-Barrientos D (2009) Divergent selection and heterogeneous genomic divergence. Mol Ecol 18:375–402.
Nunes FLD, Rigal F, Dubois SF, Viard F (2021) Looking for diversity in all the right places? Genetic diversity is highest in peripheral populations of the reef-building polychaete *Sabellaria alveolata*. Mar Biol 168:63.
Ogutu JO, Schulz-Streeck T, Piepho H-P (2012) Genomic selection using regularized linear regression models: ridge regression, lasso, elastic net and their extensions. BMC Proc 6:S10.
Oksanen J, Blanchet FG, Friendly M, Kindt R, Legendre P, McGlinn D, Minchin PR, O'Hara RB, Simpson GL, Solymos P, Stevens MHH, Szoecs E, Wagner H (2013) Package 'vegan', version 2.5-7. 1–298.
Oppliger LV, Von Dassow P, Bouchemousse S, Robuchon M, Valero M, Correa JA, Mauger S, Destombe C (2014) Alteration of sexual reproduction and genetic diversity in the kelp species *Laminaria digitata* at the southern limit of its range. PLoS ONE 9.
Paradis E, Schliep K (2019) Ape 5.0: An environment for modern phylogenetics and evolutionary analyses in R. Bioinformatics 35:526–528.
Peakall R, Smouse PE (2006) GENALEX 6: Genetic analysis in Excel. Population genetic software for teaching and research. Mol Ecol Notes 6:288–295.

909 Petton S, Garnier V, Caillaud M, Debreu L, Dumas F (2023) Using the two-way nesting
910 technique AGRIF with MARS3D V11.2 to improve hydrodynamics and estimate
911 environmental indicators. Geosci Model Dev 16:1191–1211.
912 Pingree RD, Le Cann B (1989) Celtic and Armorican slope and shelf residual currents. Prog
913 Oceanogr 23:303–338.
914 Pritchard JK, Stephens M, Donnelly P (2000) Inference of population structure using multilocus
915 genotype data. Genetics 155:945–959.
916 Pritchard JK, Wen W (2003) Documentation for STRUCTURE Software: Version 2.
917 R Core Team (2017) R: A language and environment for statistical computing.
918 Reed DC (1990) The effects of variable settlement and early competition on patterns of kelp
919 recruitment. Ecology 71:776–787.
920 Reynes L, Aurelle D, Chevalier C, Pinazo C, Valero M, Mauger S, Sartoretto S, Blanfuné A,
921 Ruitton S, Boudouresque CF, Verlaque M, Thibaut T (2021) Population genomics and
922 Lagrangian modeling shed light on dispersal events in the Mediterranean endemic *Ericaria*
923 *zosteroides* (= *Cystoseira zosteroides*) (Fucales). Front Mar Sci 8:1–18.
924 Robuchon M, Le Gall L, Mauger S, Valero M (2014) Contrasting genetic diversity patterns in
925 two sister kelp species co-distributed along the coast of Brittany, France. Mol Ecol
926 23:2669–2685.
927 Rogers-Bennett L, Catton CA (2019) Marine heat wave and multiple stressors tip bull kelp forest
928 to sea urchin barrens. Sci Rep 9:15050.
929 Roman J, Palumbi SR (2004) A global invader at home: population structure of the green crab,
930 *Carcinus maenas*, in Europe. Mol Ecol 13:2891–2898.
931 Rousset F (2008) GENEPOP'007: a complete re-implementation of the genepop software for
932 Windows and Linux. Mol Ecol Resour 8:103–106.
933 Salomon JC, Breton M (1993) An atlas of long-term currents in the Channel. Oceanol Acta
934 16:439–448.
935 Sandoval-Castillo J, Robinson NA, Hart AM, Strain LWS, Beheregaray LB (2018) Seascape
936 genomics reveals adaptive divergence in a connected and commercially important mollusc,
937 the greenlip abalone (*Haliotis laevigata*), along a longitudinal environmental gradient. Mol
938 Ecol 27:1603–1620.
939 Sanford E, Kelly MW (2011) Local adaptation in marine invertebrates. Annu Rev Mar Sci 3:509–
940 535.
941 Schoville SD, Bonin A, François O, Lobreaux S, Melodelima C, Manel S (2012) Adaptive
942 genetic variation on the landscape: Methods and cases. Annu Rev Ecol Evol Syst 43:23–
943 43.
944 Selkoe KA, Watson JR, White C, Horin TB, Iacchei M, Mitarai S, Siegel DA, Gaines SD, Toonen
945 RJ (2010) Taking the chaos out of genetic patchiness: seascape genetics reveals ecological
946 and oceanographic drivers of genetic patterns in three temperate reef species. Mol Ecol
947 19:3708–3726.
948 Sjöqvist C, Godhe A, Jonsson PR, Sundqvist L, Kremp A (2015) Local adaptation and
949 oceanographic connectivity patterns explain genetic differentiation of a marine diatom
950 across the North Sea–Baltic Sea salinity gradient. Mol Ecol 24:2871–2885.
951 Spalding MD, Fox HE, Allen GR, Davidson N, Ferdaña ZA, Finlayson M, Halpern BS, Jorge
952 MA, Lombana A, Lourie SA, Martin KD, McManus E, Molnar J, Recchia CA, Robertson
953 J (2007) Marine ecoregions of the world: A bioregionalization of coastal and shelf areas.
954 BioScience 57:573–583.
955 Starko S, Bailey LA, Creviston E, James KA, Warren A, Brophy MK, Danasel A, Fass MP,
956 Townsend JA, Neufeld CJ (2019) Environmental heterogeneity mediates scale-dependent
957 declines in kelp diversity on intertidal rocky shores. PLoS ONE 14:e0213191.
958 Teagle H, Hawkins SJ, Moore PJ, Smale DA (2017) The role of kelp species as biogenic habitat
959 formers in coastal marine ecosystems. J Exp Mar Biol Ecol 492:81–98.
960 Teske PR, Sandoval-Castillo J, Waters J, Beheregaray LB (2017) An overview of Australia's
961 temperate marine phylogeography, with new evidence from high-dispersal gastropods. J

962 Biogeogr 44:217–229.
963 Teske PR, Von Der Heyden S, McQuaid CD, Barker NP (2011) A review of marine
964 phylogeography in southern Africa. South Afr J Sci 107:43–53.
965 Treml EA, Halpin PN, Urban DL, Pratson LF (2008) Modeling population connectivity by ocean
966 currents, a graph-theoretic approach for marine conservation. Landsc Ecol 23:19–36.
967 Valero M, Destombe C, Mauger S, Ribout C, Engel CR, Daguin-Thiebaut C, Tellier F (2011)
968 Using genetic tools for sustainable management of kelps: A literature review and the
969 example of *Laminaria digitata*. Cah Biol Mar 52:467–483.
970 Van Oosterhout C, Hutchinson WF, Wills DPM, Shipley P (2004) MICRO-CHECKER: software
971 for identifying and correcting genotyping errors in microsatellite data. Mol Ecol Notes
972 4:535–538.
973 Van Oppen MJH, Coleman MA (2022) Advancing the protection of marine life through
974 genomics. PLOS Biol 20:e3001801.
975 Weir BS, Cockerham CC (1984) Estimating *F*-Statistics for the analysis of population structure.
976 Evolution 38:1358.
977 Wernberg T, Bennett S, Babcock RC, de Bettignies T, Cure K, Depczynski M, Dufois F, Fromont
978 J, Fulton CJ, Hovey RK, Harvey ES, Holmes TH, Kendrick GA, Radford B, Santana-
979 Garcon J, Saunders BJ, Smale DA, Thomsen MS, Tuckett CA, Tuya F, Vanderklift MA,
980 Wilson S (2016) Climate-driven regime shift of a temperate marine ecosystem. Science
981 353:169–172.
982 White C, Selkoe KA, Watson J, Siegel DA, Zacherl DC, Toonen RJ (2010) Ocean currents help
983 explain population genetic structure. Proc R Soc B Biol Sci 277:1685–1694.
984 Wilcox MA, Jeffery NW, DiBacco C, Bradbury IR, Lowen B, Wang Z, Beiko RG, Stanley RRE
985 (2023) Integrating seascape resistances and gene flow to produce area-based metrics of
986 functional connectivity for marine conservation planning. Landsc Ecol 38:2189–2205.
987 Xuereb A, Benestan L, Normandeau É, Daigle RM, Curtis JMR, Bernatchez L, Fortin M-J (2018)
988 Asymmetric oceanographic processes mediate connectivity and population genetic
989 structure, as revealed by RADseq, in a highly dispersive marine invertebrate
990 (*Parastichopus californicus*). Mol Ecol 27:2347–2364.
991 Xuereb A, D'Aloia CC, Daigle RM, Andrello M, Dalongeville A, Manel S, Mouillot D, Guichard
992 F, Côté IM, Curtis JMR, Bernatchez L, Fortin M-J (2019) Marine Conservation and Marine
993 Protected Areas. In: *Population Genomics: Marine Organisms*. Oleksiak MF, Rajora OP
994 (eds) Springer, Cham., p 423–446
995 Yessad K (2015) Basics about ARPEGE/IFS, ALADIN and AROME in the cycle 42 of
996 ARPEGE/IFS. Research report. Météo-France/CNRM/GMAP/ALGO.
997
998

Table 1. Information on the sampled populations: population codes as indicated in Figure 1; geographic locations (Latitude, Longitude); locality; year of sampling; position relative to the coastline; number of genotyped individuals and source of the data.

N°	Lat.	Long.	Locality	Year	Position	Nb.	Source
S1	47.339	-2.892	Hoedic	2011	Island	30	Robuchon et al. (2014)
S2	47.394	-2.958	Houat	2011	Island	30	Robuchon et al. (2014)
S3	47.328	-3.124	Belle-île	2006	Island	30	This study
S4	47.470	-3.091	Quiberon	2008	Coastline	28	This study
S5	47.762	-3.549	Lorient	2006	Coastline	24	Valero et al. (2011)
S6	47.791	-3.761	Pont Aven	2006	Coastline	28	Valero et al. (2011)
S7	47.700	-3.983	Glénan	2008	Island	30	This study
S8	47.786	-4.152	Loctudy	2008	Coastline	20	This study
S9	47.799	-4.383	Penmarc'h	2006	Coastline	29	Valero et al. (2011)
S10	48.032	-4.835	Ile de Sein	2009	Island	24	This study
S11	48.284	-4.601	Crozon	2011	Coastline	30	This study
S12	48.326	-4.764	Le Conquet	2011	Coastline	30	Robuchon et al. (2014)
S13	48.381	-4.919	Le Conquet	2011	Island	30	Robuchon et al. (2014)
S14	48.519	-4.779	Porspoder	2003	Coastline	25	Robuchon et al. (2014)
S15	48.673	-4.216	Plouescat	2005	Coastline	30	Valero et al. (2011)
S16	48.700	-4.152	Téven-Meur	2011	Coastline	30	Robuchon et al. (2014)
S17	48.711	-4.060	Ile de Sieck	2005	Coastline	30	Valero et al. (2011)
S18	48.725	-3.919	Roscoff	2011	Coastline	30	Robuchon et al. (2014)
S19	48.721	-3.803	Plougasnou	2011	Coastline	30	Robuchon et al. (2014)
S20	48.775	-3.777	Plateau de la Méloine	2015	Island	26	This study
S21	48.687	-3.613	Locquirec	2006	Coastline	27	Valero et al. (2011)
S22	48.871	-3.643	Triagoz	2012	Island	27	This study
S23	48.878	-3.513	Trégastel	2006	Island	27	This study
S24	48.881	-3.099	Tréguier	2006	Coastline	20	This study
S25	49.118	-2.821	Roche Douvres	2012	Island	26	This study

S26	48.688	-2.325	Plévenon	2011	Coastline	30	Robuchon et al. (2014)
S27	48.651	-2.118	Saint-Lunaire	2011	Coastline	30	Robuchon et al. (2014)
S28	48.694	-1.984	Saint-Malo	2011	Coastline	29	Robuchon et al. (2014)
S29	48.697	-1.919	Saint-Malo	2006	Coastline	27	This study
S30	49.729	-1.919	Omonville	2006	Coastline	29	This study
S31	49.653	-1.234	Barfleur	2006	Coastline	30	This study
S32	50.912	1.677	Wissant	2006	Coastline	30	This study

1003

1004

Table 2. F_{ST} values averaged across all pairwise comparisons ($\overline{F_{ST}}$) for the samples or the group of samples mentioned in the first column. When the first column indicates a group of samples (which correspond to a genetic cluster, see Figure 2), the F_{ST} was additionally averaged across the populations belonging to that group. The populations or groups of populations from the southernmost populations (S1-S4); Locquirec (S21); populations from Saint-Malo Bay (S26-S29) and Dover Strait (S32) appeared to be particularly differentiated, as shown by higher $\overline{F_{ST}}$ compared to the rest of the populations (last line, "Others"). Minimum and maximum $\overline{F_{ST}}$ values are also indicated. The full pairwise F_{ST} matrix can be found in Table S5.

Samples or group of samples	$\overline{F_{ST}}$	***FST* min**	***FST* max**
S1-S4	0.183	0.024	0.395
S21	0.168	0.107	0.317
S26-S29	0.144	0.019	0.395
S32	0.227	0.159	0.356
Others	0.08	0.01	0.23

Table 3. Estimates of genetic diversity associated to each population using *Ho*: observed heterozygosity, *He*: expected heterozygosity, *Ar*: allelic richness (calculated with minimum 19 diploid individuals), $\overline{Pa}$ *:* mean private alleles and deviation from Hardy-Weinberg Equilibrium estimated using F_{IS}, ***** when the deviation is significant (p-value < 0.001, based on 1,000 permutations using GENETIX).

N°	Position	*Ho*	*He*	*Ar*	$\overline{Pa}$	F_{IS}
S1	Island	0.552 ± 0.065	0.541 ± 0.055	3.724 ± 0.406	0 ± 0	-0.002
S2	Island	0.49 ± 0.051	0.51 ± 0.051	3.543 ± 0.304	0 ± 0	0.057
S3	Island	0.43 ± 0.068	0.425 ± 0.067	3.595 ± 0.31	0.091 ± 0.091	0.003
S4	Coastline	0.432 ± 0.072	0.426 ± 0.063	3.733 ± 0.452	0.091 ± 0.091	0.003
S5	Coastline	0.547 ± 0.066	0.555 ± 0.053	5.05 ± 0.684	0 ± 0	0.035
S6	Coastline	0.551 ± 0.066	0.539 ± 0.05	4.67 ± 0.584	0.091 ± 0.091	-0.004
S7	Island	0.539 ± 0.062	0.565 ± 0.051	5.22 ± 0.68	0.091 ± 0.091	0.063 *
S8	Coastline	0.586 ± 0.052	0.579 ± 0.05	5.554 ± 1.014	0.182 ± 0.182	0.013
S9	Coastline	0.513 ± 0.055	0.549 ± 0.05	5.443 ± 0.769	0.182 ± 0.182	0.083 *
S10	Island	0.561 ± 0.054	0.596 ± 0.05	5.913 ± 0.854	0 ± 0	0.08 *
S11	Coastline	0.555 ± 0.067	0.62 ± 0.065	5.551 ± 0.995	0.091 ± 0.091	0.122 *
S12	Coastline	0.561 ± 0.051	0.609 ± 0.055	6.151 ± 0.87	0.455 ± 0.207	0.097 *
S13	Island	0.552 ± 0.06	0.576 ± 0.062	5.613 ± 0.859	0 ± 0	0.06 *
S14	Coastline	0.585 ± 0.063	0.582 ± 0.054	6.004 ± 0.812	0.182 ± 0.122	0.014
S15	Coastline	0.617 ± 0.063	0.584 ± 0.059	5.355 ± 0.989	0 ± 0	-0.038
S16	Coastline	0.526 ± 0.06	0.555 ± 0.062	5.404 ± 0.898	0 ± 0	0.07 *
S17	Coastline	0.561 ± 0.073	0.543 ± 0.07	5.476 ± 0.99	0.091 ± 0.091	-0.015
S18	Coastline	0.495 ± 0.073	0.508 ± 0.078	4.814 ± 0.809	0.091 ± 0.091	0.043
S19	Coastline	0.445 ± 0.081	0.488 ± 0.074	4.451 ± 0.699	0.091 ± 0.091	0.103 *
S20	Island	0.418 ± 0.077	0.426 ± 0.076	3.942 ± 0.734	0.091 ± 0.091	0.04
S21	Coastline	0.387 ± 0.072	0.376 ± 0.066	3.158 ± 0.456	0 ± 0	-0.01
S22	Island	0.461 ± 0.087	0.471 ± 0.09	4.482 ± 1.077	0 ± 0	0.04

S23	Island	0.465 ± 0.095	0.452 ± 0.09	4.483 ± 0.927	0.273 ± 0.141	-0.01
S24	Coastline	0.496 ± 0.086	0.486 ± 0.078	4.508 ± 0.832	0.182 ± 0.122	0.006
S25	Island	0.457 ± 0.08	0.485 ± 0.078	3.762 ± 0.626	0 ± 0	0.078 *
S26	Coastline	0.33 ± 0.083	0.347 ± 0.082	3.361 ± 0.679	0.091 ± 0.091	0.064
S27	Coastline	0.45 ± 0.08	0.403 ± 0.07	2.951 ± 0.532	0 ± 0	-0.1 *
S28	Coastline	0.426 ± 0.078	0.382 ± 0.062	3.22 ± 0.431	0.091 ± 0.091	-0.098 *
S29	Coastline	0.424 ± 0.078	0.423 ± 0.068	3.271 ± 0.58	0.091 ± 0.091	0.017
S30	Coastline	0.448 ± 0.086	0.454 ± 0.076	4.361 ± 0.846	0 ± 0	0.03
S31	Coastline	0.487 ± 0.091	0.477 ± 0.078	4.414 ± 0.812	0 ± 0	-0.003
S32	Coastline	0.308 ± 0.083	0.29 ± 0.073	2.542 ± 0.407	0 ± 0	-0.046

1023

Table 4. Results of the partial and global db-RDA for each dataset: overall (32 populations), regional (29 populations) and continuous datasets (24 populations). Environmental predictors selected by the stepwise forward selection (ordiR2step) are included in the db-RDA framework, the predictors highlighted in bold are significant at $p < 0.001$ according to the ANOVA. The adjusted coefficient of determination (R^2_{adj}) and the *p*-value of the model are reported. Habitat continuity and sampling year were not selected as a significant predictor in the global nor partial db-RDA and are therefore not represented in this table.

Overall	Oceanographic Connectivity	Geographic Position	Sea Surface Temperature	*p*-value	R^2_{adj}
Global db-RDA	AEM1, AEM3, AEM26, AEM2	dbMEM1, dbMEM3, dbMEM5		0.001	0.604
Partial db-RDA	AEM7, AEM6, AEM26			0.012	0.115
		dbMEM1, dbMEM3, dbMEM5		0.001	0.475
			Mean, Min	0.002	0.165
Regional					
Global db-RDA	AEM23, AEM2, AEM1, AEM25	dbMEM2, dbMEM3		0.001	0.614
Partial db-RDA	AEM2, AEM1, AEM23, AEM25, AEM7, AEM6, AEM9			0.001	0.549
		dbMEM2, dbMEM3, dbMEM1		0.001	0.485
			Mean, Min, Max, Range	0.001	0.221
Continuous					
Global db-RDA	AEM1, AEM2, AEM16, AEM10, AEM5, AEM19, AEM3	dbMEM3		0.001	0.748
Partial db-RDA	AEM1, AEM2, AEM16, AEM10, AEM5, AEM19, AEM3, AEM20, AEM9, AEM7			0.001	0.794
		dbMEM2, dbMEM3, dbMEM1		0.001	0.513
			Max	0.003	0.210

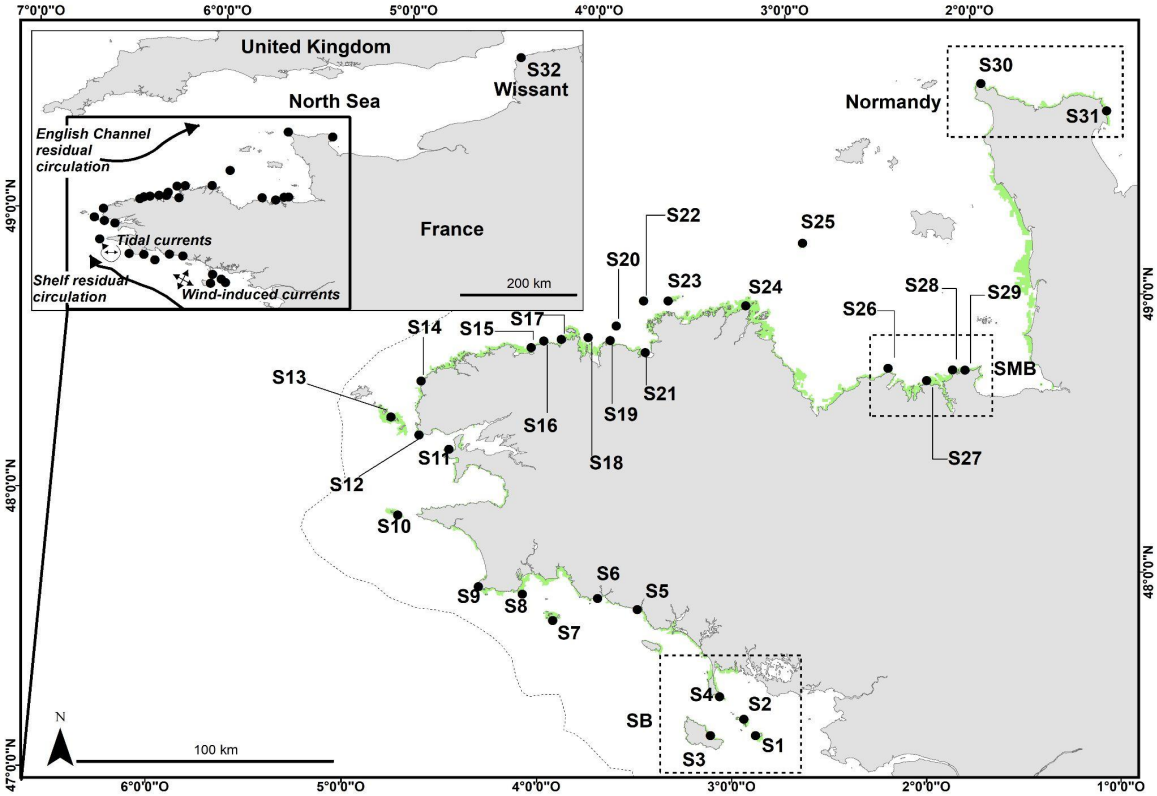

Figure 1. Geographic position of the sampled populations, the Northernmost site (S32) is indicated in the inset. Population numbers correspond to the ones indicated in Table 1 and the area illustrated in green corresponds to rocky substrata above 5m depth obtained from IFREMER in May 2019. The information on the spatial distribution of bedrock comes from the combination of several sources as specified in the Material and Method section. The dotted line corresponds to the 120m isobath, which could correspond to the coastline at the Last Glacial Maximum. The inset illustrates the general circulation in the Bay of Biscay and in the English Channel, drawn according to Ayata et al. (2010).

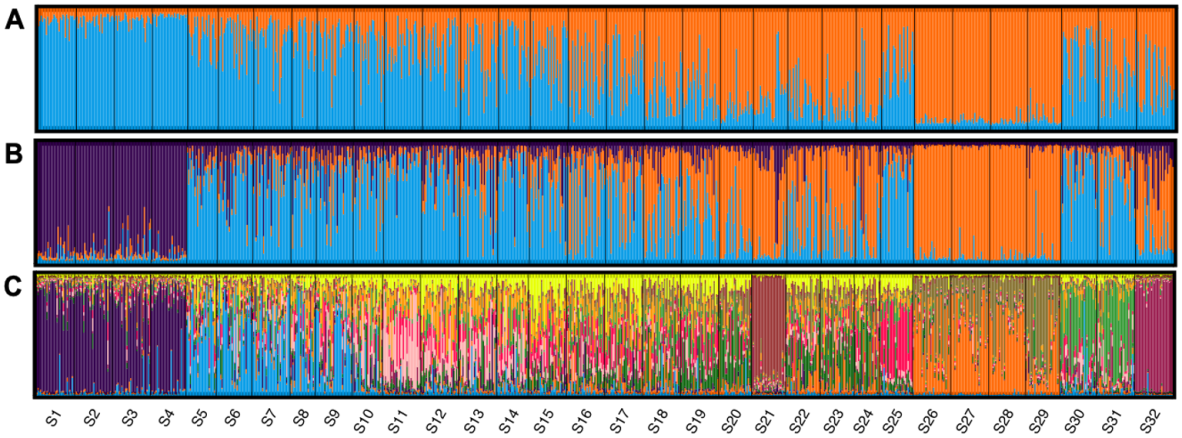

Figure 2. STRUCTURE barplot obtained for K = 2 (**A**), K = 3 (**B**) and K = 12 (**C**) which appeared the best number of clusters according to both ΔK and log Pr(X|K) methods. Each vertical bar corresponds to one individual and the colors represent the individual's estimated proportion of ancestry in each of the K clusters. The numbers below correspond to the population code as indicated in Table and Figure 1.

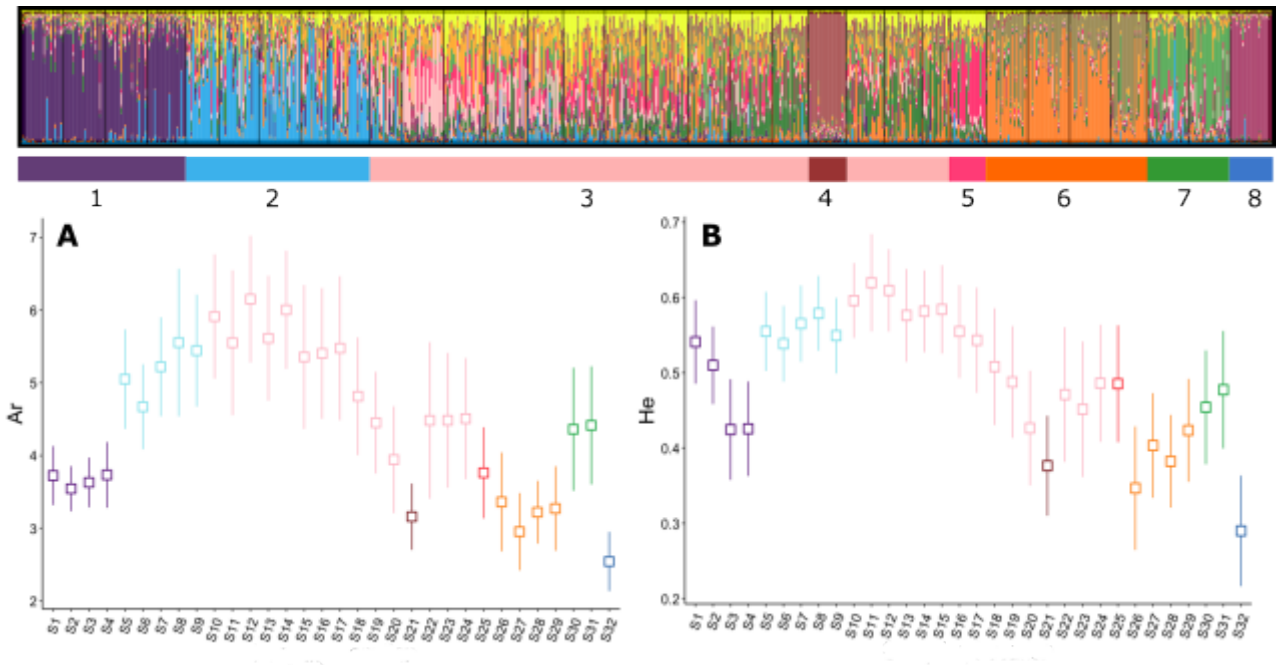

Figure 3. **A.** Allelic richness (*Ar*) and **B.** Expected heterozygosity (*He*) observed among the 32 populations. The colors of the plots correspond to the eight genetic groups illustrated with the STRUCTURE barplot above. These figures illustrate the average and the standard deviation observed across markers.

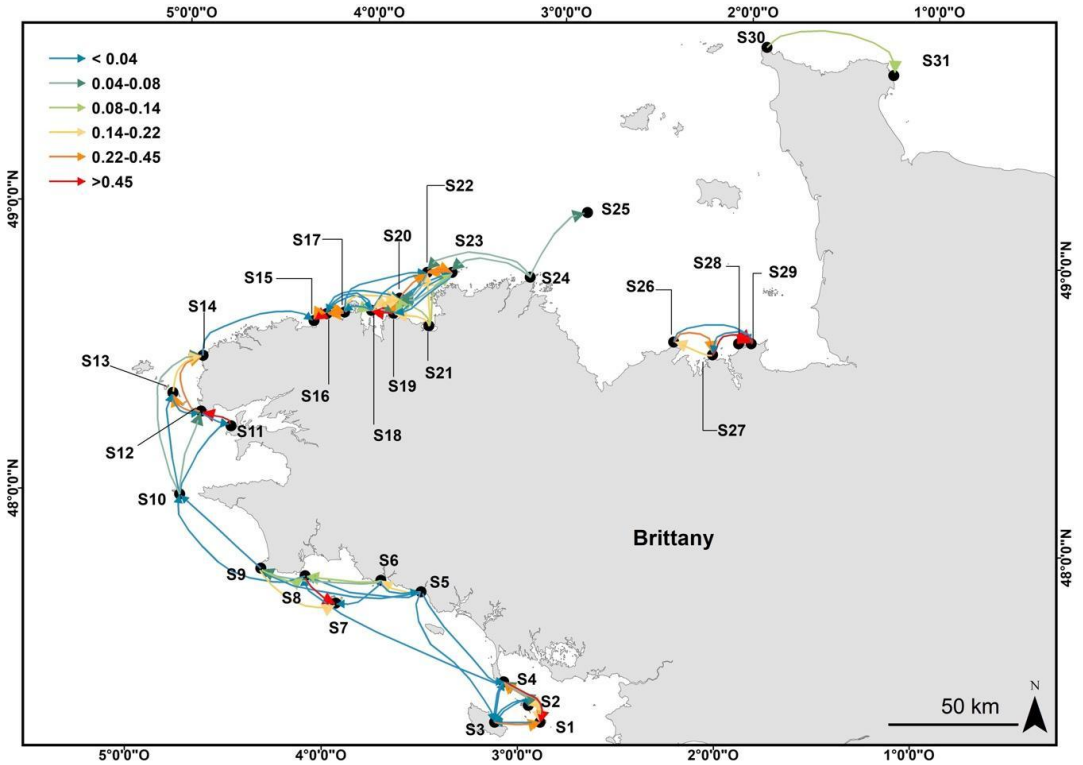

Figure 4. Map illustrating the probability of connectivity obtained from the Lagrangian simulation model. The color gradient is located on the top left corner: cold color indicates low connectivity while warm color indicates high connectivity. For the clarity of the figure, values below 10^{-2} are not represented.

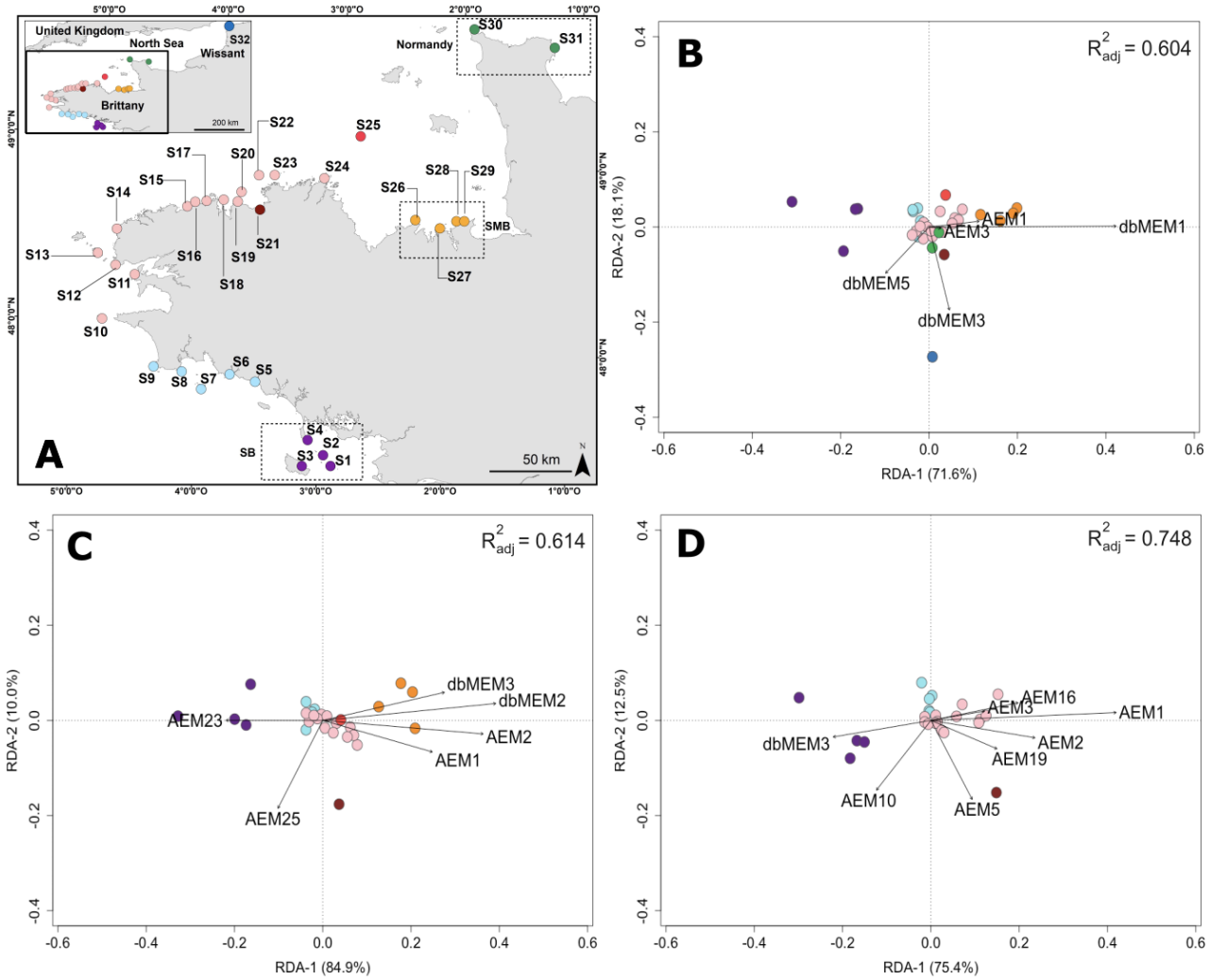

Figure 5. Figure A. Geographic position of the sampled populations. The color used for each population corresponds to the genetic clusters illustrated in Figure 3. Figures **B**. **C** and **D** represent the results of the global db-RDA at the **B**. overall (32 populations), **C**. regional (29 populations) and **D**. continuous scale (24 populations). The numbers written in brackets on each axis correspond to the percentage of variance explained by each axis. The black arrows illustrate the relative contribution of the significant environmental factors according to the ANOVA and the stepwise forward selection (ordiR2step) process. The length of the arrows illustrates the relative contribution of each environmental predictor: as the length of the arrow increases, the contribution of the environmental predictor in explaining the neutral genetic variation increases. The adjusted coefficient of determination (R^2_{adj}) of each model is reported on the top right corner.

APPENDIX

Table S1. Genetic data of the 12 *Laminaria hyperborea* individuals that were found in our dataset and were then discarded.

		Ld148		Ld158		Ld167		Ld371		Ld531		Ld704		Lo454-23		Lo454-24		Lo454-17		Lo454-28		Lo4-24	
Individual_code	Population	Allele 1	Allele 2	Allele 1	Allele 2	Allele 1	Allele 2	Allele 1	Allele 2	Allele 1	Allele 2	Allele 1	Allele 2	Allele 1	Allele 2	Allele 1	Allele 2	Allele 1	Allele 2	Allele 1	Allele 2	Allele 1	Allele 2
LD_SB2_T2_03	S6	198	198	240	240	173	176	120	123	236	239	288	290	214	223	286	289	180	180	222	222	218	218
LD_SB2_T2_04	S6	198	198	238	240	173	173	123	126	233	245	288	292	223	226	280	289	165	165	222	222	218	218
LD_SB3_T2_20	S9	189	198	240	242	173	173	120	132	236	242	288	288	214	214	268	280	165	165	234	258	164	164
LD_NB4B_T2_14	S21	195	195	240	242	176	176	120	123	242	242	286	288	199	211	268	268	180	180	234	234	216	216
LD_NB4B_T2_18	S21	183	183	238	240	173	176	120	123	236	242	290	292	211	211	268	283	180	180	258	258	216	216
LD_NB4B_T2_20	S21	186	198	240	240	176	176	123	132	236	242	288	292	211	211	268	280	180	180	234	258	216	216
LD_TRIA_12_09	S22	207	240	222	222	146	152	141	147	200	200	340	342	196	214	268	283	165	168	222	246	216	216
LD_TRIA_12_13	S22	240	249	222	222	152	158	147	153	200	200	0	0	214	214	268	289	165	165	234	246	164	216
LD_TRIA_12_14	S22	237	237	222	228	146	155	141	150	200	200	342	402	214	223	286	286	168	180	246	258	216	216
LD_RD_12_03	S25	207	240	222	222	155	155	117	150	200	200	348	350	214	214	268	289	165	165	222	258	216	216
LD_BIG_7	S28	198	198	238	240	170	170	120	144	304	316	233	242	316	316	304	316	180	180	206	206	224	224
LD_NO1_T2_15	S30	186	195	240	240	173	176	126	144	236	239	288	292	214	223	268	268	165	198	222	222	218	218

Table S2. Frequency of null alleles per marker and per population of *Laminaria digitata* obtained using FREENA (Chapuis & Estoup 2007) software. Significant values (>0.05) are highlighted in bold.

	1	2	3	4	5	6	7	8	9	10	11
S1	0.00000	**0.14116**	0.00000	0.00002	0.00003	0.00001	0.00000	0.01660	0.00000	0.00000	0.00003
S2	0.02774	**0.14453**	0.00914	0.01429	0.00176	0.00000	0.09697	0.00000	0.01186	0.00000	0.00001
S3	0.00000	0.00000	0.00000	0.04868	0.02706	0.00001	0.00000	0.00006	0.00027	0.00001	0.00001
S4	0.00003	0.00000	0.00001	0.00000	0.00001	0.03180	0.00000	0.00002	0.00001	0.02489	**0.12131**
S5	0.00000	0.00001	0.00000	0.00003	0.00001	0.00001	**0.05281**	**0.12178**	0.00000	0.00998	**0.12604**
S6	0.00001	0.01403	0.00000	0.02359	0.00000	0.00000	0.00000	**0.06157**	0.00010	**0.06567**	0.04787
S7	0.00002	**0.22978**	**0.07437**	0.00000	0.04443	0.01515	**0.06585**	0.00001	0.00000	0.00000	0.01234
S8	0.00000	**0.10478**	0.00000	0.01417	**0.05713**	0.00004	0.00001	0.00000	0.00001	0.00000	0.02857
S9	0.00000	0.02682	0.02117	0.01277	0.01499	**0.07276**	0.00001	0.03514	0.00000	**0.08371**	0.04428
S10	0.02275	**0.10738**	0.00000	0.00002	0.00669	0.01254	**0.15491**	0.00000	**0.05791**	0.00000	**0.06169**
S11	0.00000	0.01554	0.01249	0.03615	**0.07386**	**0.07288**	**0.19612**	0.00000	**0.07836**	**0.06999**	0.00001
S12	0.00000	**0.05742**	0.05824	0.05760	0.00000	**0.09358**	**0.10696**	0.00000	0.01317	0.05477	0.00000
S13	0.00003	0.01514	**0.09196**	0.00000	0.04064	0.00001	**0.09185**	0.00000	0.03628	0.00380	0.04258
S14	0.00000	0.00000	0.04776	0.00000	0.00000	0.00000	0.00001	0.00000	0.00001	**0.14995**	0.00000
S15	0.01337	**0.05210**	0.04766	0.00000	0.00000	0.00000	0.00000	0.00001	0.00000	0.00001	0.00001
S16	0.03932	0.03397	0.00001	0.01703	0.01464	0.00001	**0.06292**	**0.05912**	**0.05874**	0.00000	0.00001
S17	0.04793	0.00001	0.00001	0.00000	0.00000	0.00001	0.00000	0.00683	0.00001	0.04340	0.00001
S18	0.00000	0.00000	0.00377	0.03195	0.03602	0.00003	0.01581	0.00000	0.00000	**0.05729**	0.00006
S19	0.06208	**0.11020**	**0.10713**	0.00000	0.00000	0.00001	0.05086	0.00017	0.00000	**0.14337**	0.00003
S20	**0.08324**	**0.06339**	0.00000	0.00000	**0.06476**	0.00001	0.00000	0.00000	0.00002	0.00000	0.04129
S21	0.00000	0.00000	0.08722	0.00000	0.01225	0.00000	0.00001	0.00000	**0.05202**	0.00002	0.00100
S22	0.00918	0.04703	0.00001	0.00701	0.02473	0.00001	**0.06987**	0.00001	0.00001	0.00002	0.00100
S23	0.00000	0.00000	0.10286	0.00196	0.00001	0.00002	0.00000	0.00772	0.00002	0.00000	0.00005
S24	0.00000	0.00000	0.00000	0.00000	0.05630	0.00000	0.00000	0.00000	**0.13000**	0.00000	**0.14934**
S25	0.00000	**0.05569**	**0.09105**	**0.06130**	**0.12111**	0.00002	0.00000	0.00000	0.00000	**0.10687**	0.00005
S26	0.00000	**0.07512**	0.01105	**0.05541**	0.03104	**0.11411**	0.04832	0.00035	0.00100	0.00001	0.00100
S27	0.00000	0.00000	0.00012	0.00000	0.00002	0.00040	0.00000	0.00000	0.00100	0.00001	0.00006
S28	0.00000	0.00005	0.00000	0.00000	0.02300	**0.05556**	0.00000	0.00000	0.00003	0.02259	0.00100
S29	0.00014	0.00001	0.02214	0.00000	0.00587	0.00001	0.02941	**0.07881**	0.00142	**0.11415**	0.00100
S30	0.01765	0.00003	0.04487	0.00000	0.00001	0.00000	0.01796	**0.06386**	**0.05004**	0.00002	**0.12557**
S31	**0.06137**	0.00002	0.00000	0.00000	0.01193	0.00000	0.02918	**0.09089**	**0.11065**	0.00001	0.00100
S32	0.00000	0.01301	0.00001	0.00000	0.00000	**0.06892**	0.00001	0.00006	0.00100	0.00100	0.00100

Table S3. Test on linkage disequilibrium calculated across populations using Genepop 4.7.5 (Rousset 2008). The *p*-value was obtained using the log likelihood ratio statistic. The Markov chain parameters were: dememorization number 1,000, number of batches 100 and number of iterations per batch 1,000. The column df corresponds to the degrees of freedom. The same test has been performed at the individual-level, however, due to the size of the results (about 1680 rows) only the results obtained at the population-level are shown here.

Pair of locus	Chi2	df	*p*-value
Ld148 & Ld158	61.268593	64	0.573686
Ld148 & Ld167	42.493175	64	0.982484
Ld158 & Ld167	52.435867	64	0.848782
Ld148 & Ld371	54.364079	64	0.799238
Ld158 & Ld371	78.148001	64	0.109978
Ld167 & Ld371	50.098955	64	0.898109
Ld148 & Ld531	57.592577	64	0.700887
Ld158 & Ld531	61.404635	64	0.568834
Ld167 & Ld531	70.589502	64	0.266955
Ld371 & Ld531	39.414769	64	0.993362
Ld148 & Ld704	54.058741	64	0.807589
Ld158 & Ld704	61.528524	64	0.564413
Ld167 & Ld704	58.719018	64	0.663082
Ld371 & Ld704	77.932809	64	0.113144
Ld531 & Ld704	52.639406	64	0.843920
Ld148 & Lo454-23	47.407483	64	0.940200
Ld158 & Lo454-23	49.175046	64	0.914295
Ld167 & Lo454-23	38.753006	64	0.994736
Ld371 & Lo454-23	63.802023	64	0.483462
Ld531 & Lo454-23	58.601617	64	0.667085
Ld704 & Lo454-23	67.105332	64	0.371118
Ld148 & Lo454-24	46.519072	64	0.950850
Ld158 & Lo454-24	65.551027	64	0.422754
Ld167 & Lo454-24	69.728007	64	0.290998
Ld371 & Lo454-24	50.786090	64	0.884856
Ld531 & Lo454-24	62.019929	64	0.546860
Ld704 & Lo454-24	50.406460	64	0.892307
Lo454-23 & Lo454-24	68.470619	64	0.328181
Ld148 & Lo454-17	47.841024	58	0.826859
Ld158 & Lo454-17	74.338907	58	0.072860
Ld167 & Lo454-17	58.110128	58	0.471238
Ld371 & Lo454-17	37.051539	58	0.985433
Ld531 & Lo454-17	45.415862	58	0.885395
Ld704 & Lo454-17	42.039292	58	0.943114
Lo454-23 & Lo454-17	43.715190	58	0.917860
Lo454-24 & Lo454-17	45.470829	58	0.884227
Ld148 & Lo454-28	62.806792	62	0.447496
Ld158 & Lo454-28	53.613270	62	0.767138
Ld167 & Lo454-28	80.045575	62	0.061275
Ld371 & Lo454-28	77.249968	62	0.091798
Ld531 & Lo454-28	63.153229	62	0.435358
Ld704 & Lo454-28	48.081654	62	0.902663
Lo454-23 & Lo454-28	54.884311	62	0.727320
Lo454-24 & Lo454-28	33.594225	62	0.998792
Lo454-17 & Lo454-28	72.616313	58	0.093731
Ld148 & Lo4-24	26.784328	50	0.997090
Ld158 & Lo4-24	29.536432	50	0.990630
Ld167 & Lo4-24	53.755514	50	0.332557
Ld371 & Lo4-24	40.193247	50	0.837790
Ld531 & Lo4-24	33.543912	50	0.964280
Ld704 & Lo4-24	45.591302	50	0.650735
Lo454-23 & 4-24	43.829326	50	0.718035
Lo454-24 & 4-24	47.048043	50	0.592566
Lo454-17 & 4-24	39.936610	48	0.789608
Lo454-28 & 4-24	45.021258	50	0.672971

Table S4 Pairwise F_{ST} values calculated according to Weir & Cockerham (1984) using GENETIX (below the diagonal) and their significance calculated with 1,000 permutations using the same software (above the diagonal). The adjusted *p*-value obtained for multiple comparisons is: 0.0001. ** when *p*-value < 0.00001, * when *p*-value < 0.0001, NS when non-significant.

	S1	S2	S3	S4	S5	S6	S7	S8	S9	S10	S11	S12	S13	S14	S15	S16	S17	S18	S19	S20	S21	S22	S23	S24	S25	S26	S27	S28	S29	S30	S31	S32
S1		NS	**	**	**	**	**	**	**	**	**	**	**	**	**	**	**	**	**	**	**	**	**	**	**	**	**	**	**	**	**	**
S2	0.024		**	**	**	**	**	**	**	*	**	**	**	**	**	**	**	**	**	**	**	**	**	**	**	**	**	**	**	**	**	**
S3	0.088	0.081		**	**	**	**	**	**	NS	**	**	**	**	**	**	**	**	**	**	**	**	**	**	**	**	**	**	**	**	**	**
S4	0.127	0.106	0.129		**	**	**	**	**	**	**	**	**	**	**	**	**	**	**	**	**	**	**	**	**	**	**	**	**	**	**	**
S5	0.139	0.134	0.144	0.197		NS	NS	NS	NS	NS	**	**	**	NS	**	**	**	**	**	**	**	**	**	**	**	**	**	**	**	**	**	**
S6	0.148	0.127	0.141	0.181	0.012		**	*	**	**	**	**	**	**	**	**	**	**	**	**	**	**	**	**	**	**	**	**	**	**	**	**
S7	0.141	0.136	0.133	0.182	0.017	0.023		NS	NS	*	**	**	**	**	**	*	**	**	**	**	**	**	**	**	**	**	**	**	**	**	**	**
S8	0.11	0.114	0.123	0.185	0.012	0.022	0.016		NS	NS	**	NS	NS	NS	NS	NS	NS	*	**	**	**	**	**	**	**	**	**	**	**	**	**	**
S9	0.133	0.135	0.11	0.194	0.015	0.041	0.024	0.004		NS	**	**	**	NS	NS	NS	**	**	**	**	**	**	**	**	**	**	**	**	**	**	**	**
S10	0.11	0.096	0.115	0.153	0.018	0.024	0.026	0.007	0.017		**	NS	NS	NS	NS	NS	**	**	**	**	**	**	**	**	**	**	**	**	**	**	**	**
S11	0.12	0.124	0.145	0.195	0.083	0.079	0.08	0.054	0.074	0.039		NS	**	**	**	**	**	**	**	**	**	**	**	**	**	**	**	**	**	**	**	**
S12	0.115	0.109	0.149	0.189	0.042	0.042	0.05	0.02	0.036	0.005	0.022		NS	NS	NS	NS	NS	NS	**	**	**	**	**	**	**	**	**	**	**	**	**	**
S13	0.113	0.111	0.139	0.195	0.047	0.052	0.05	0.019	0.03	0.004	0.042	0.001		NS	NS	NS	NS	*	**	**	**	NS	**	**	**	**	**	**	**	**	**	**
S14	0.12	0.122	0.12	0.199	0.017	0.032	0.035	0.005	0.006	0.001	0.03	0.006	0.013		NS	NS	NS	**	**	**	**	**	**	**	**	**	**	**	**	**	**	**
S15	0.093	0.092	0.129	0.174	0.046	0.054	0.062	0.022	0.042	0.01	0.047	0.011	0.01	0.018		NS	NS	**	**	**	**	**	**	**	**	**	**	**	**	**	**	**
S16	0.114	0.111	0.136	0.209	0.038	0.053	0.058	0.019	0.036	0.012	0.059	0.019	0.008	0.018	0.006		NS	NS	**	**	**	**	**	*	**	**	**	**	**	**	**	**
S17	0.126	0.111	0.155	0.202	0.066	0.058	0.083	0.04	0.065	0.021	0.056	0.015	0.011	0.03	0.007	0.007		*	**	**	**	**	**	*	**	**	**	**	**	**	**	**
S18	0.159	0.138	0.167	0.228	0.059	0.062	0.06	0.03	0.049	0.018	0.072	0.027	0.019	0.028	0.029	0.012	0.018		NS	**	**	NS	NS	NS	**	**	**	**	**	**	**	**
S19	0.172	0.144	0.209	0.235	0.101	0.096	0.111	0.072	0.104	0.047	0.095	0.039	0.033	0.071	0.036	0.037	0.024	0.019		**	**	**	NS	NS	**	**	**	**	**	**	**	**
S20	0.222	0.195	0.233	0.291	0.071	0.069	0.099	0.066	0.082	0.046	0.132	0.059	0.046	0.065	0.056	0.041	0.04	0.029	0.052		**	**	NS	NS	**	**	**	**	**	**	**	**
S21	0.243	0.221	0.214	0.317	0.165	0.153	0.188	0.151	0.149	0.131	0.16	0.137	0.131	0.127	0.137	0.119	0.111	0.124	0.164	0.135		**	**	**	**	**	**	**	**	**	**	**
S22	0.176	0.172	0.21	0.27	0.083	0.095	0.103	0.056	0.068	0.036	0.1	0.039	0.026	0.046	0.044	0.033	0.028	0.017	0.044	0.037	0.124		NS	NS	**	**	**	**	**	**	**	**
S23	0.192	0.175	0.213	0.278	0.085	0.083	0.097	0.058	0.079	0.043	0.107	0.043	0.029	0.057	0.047	0.028	0.023	0.005	0.02	0.016	0.121	0.006		NS	**	**	**	**	**	**	**	**
S24	0.178	0.167	0.205	0.265	0.083	0.082	0.097	0.056	0.076	0.038	0.08	0.031	0.026	0.046	0.038	0.028	0.017	0.011	0.022	0.019	0.107	0.013	-0.005		**	**	**	**	**	**	**	**
S25	0.187	0.167	0.211	0.268	0.068	0.069	0.085	0.042	0.081	0.048	0.086	0.035	0.044	0.047	0.041	0.045	0.046	0.035	0.045	0.056	0.185	0.06	0.05	0.055		**	**	**	**	**	**	**
S26	0.298	0.292	0.312	0.391	0.142	0.153	0.161	0.125	0.136	0.123	0.187	0.131	0.104	0.123	0.123	0.083	0.101	0.059	0.12	0.068	0.189	0.068	0.057	0.085	0.121		**	**	**	**	**	**
S27	0.239	0.272	0.284	0.387	0.164	0.181	0.168	0.125	0.133	0.132	0.157	0.113	0.093	0.117	0.117	0.083	0.106	0.096	0.155	0.135	0.211	0.084	0.103	0.104	0.154	0.086		NS	**	**	**	**
S28	0.264	0.285	0.31	0.395	0.17	0.185	0.174	0.136	0.161	0.137	0.182	0.13	0.109	0.138	0.123	0.082	0.105	0.08	0.136	0.122	0.225	0.088	0.087	0.098	0.15	0.057	0.019		**	**	**	**
S29	0.228	0.224	0.242	0.337	0.122	0.125	0.114	0.087	0.119	0.105	0.134	0.108	0.096	0.102	0.1	0.064	0.088	0.046	0.114	0.091	0.184	0.089	0.068	0.077	0.096	0.048	0.074	0.055		**	**	**
S30	0.203	0.177	0.21	0.261	0.066	0.067	0.083	0.056	0.071	0.037	0.084	0.045	0.052	0.036	0.075	0.054	0.062	0.04	0.066	0.087	0.189	0.076	0.072	0.073	0.06	0.147	0.184	0.182	0.137		**	**
S31	0.182	0.168	0.172	0.249	0.07	0.08	0.069	0.056	0.062	0.036	0.068	0.05	0.059	0.029	0.076	0.053	0.076	0.043	0.086	0.107	0.188	0.092	0.089	0.077	0.09	0.164	0.158	0.168	0.119	0.025		**
S32	0.284	0.278	0.229	0.356	0.245	0.239	0.246	0.206	0.183	0.179	0.203	0.205	0.189	0.168	0.186	0.159	0.178	0.18	0.24	0.248	0.207	0.225	0.221	0.214	0.273	0.284	0.267	0.278	0.248	0.223	0.189	

Table S5. Habitat discontinuity estimated by the proportion of the geographic distance unoccupied by rocky substrata (values are the same below and above the diagonal). The color gradient illustrates whether the proportion gets near to 1 (dark blue, complete habitat discontinuity) or 0 (white, no habitat discontinuity), which means that the distance separating the pair of populations is completely occupied by rocky substrate above 5m depth).

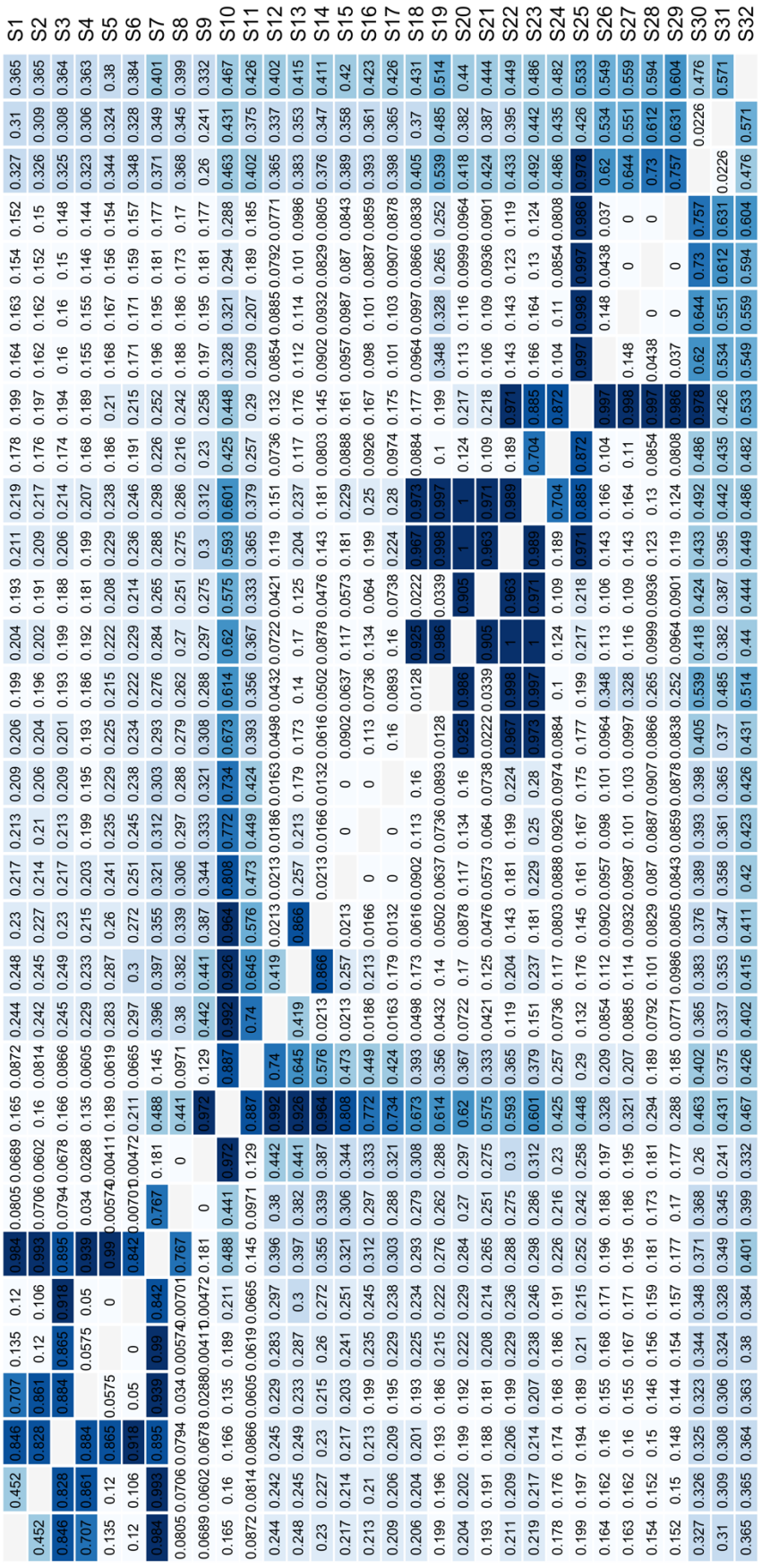

Table S6. Average probability of connectivity between release (column) and recruitment area (row). The probability is averaged between results obtained for year 2014 and 2015. The color gradient indicates when the probability tends towards 1 (dark blue) or 0 (white). The values were rounded at 10^{-3}, therefore 0 indicates values between 10^{-7} and 10^{-3}; whereas grey cells without values indicate true zero probability of connectivity.

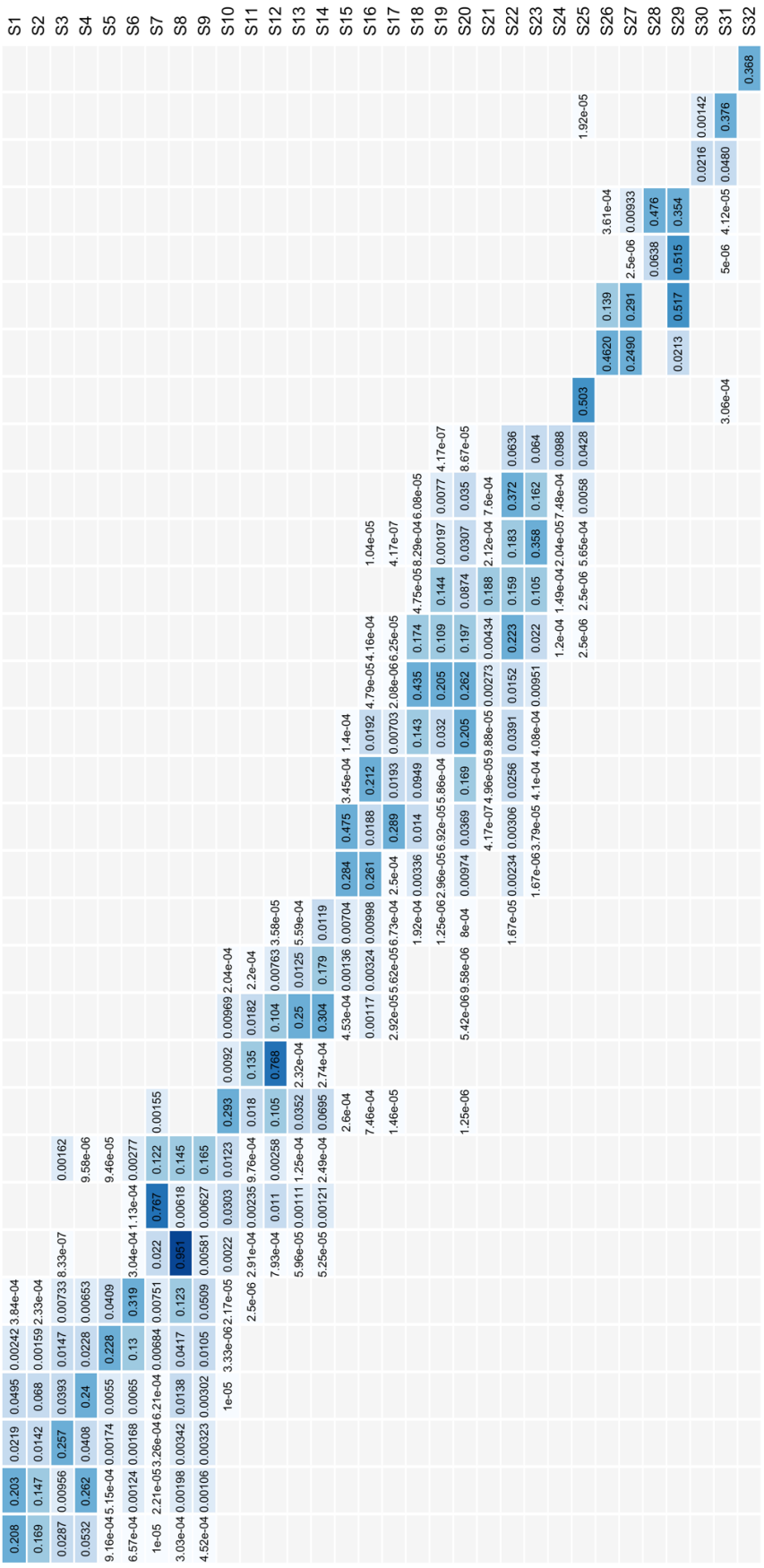

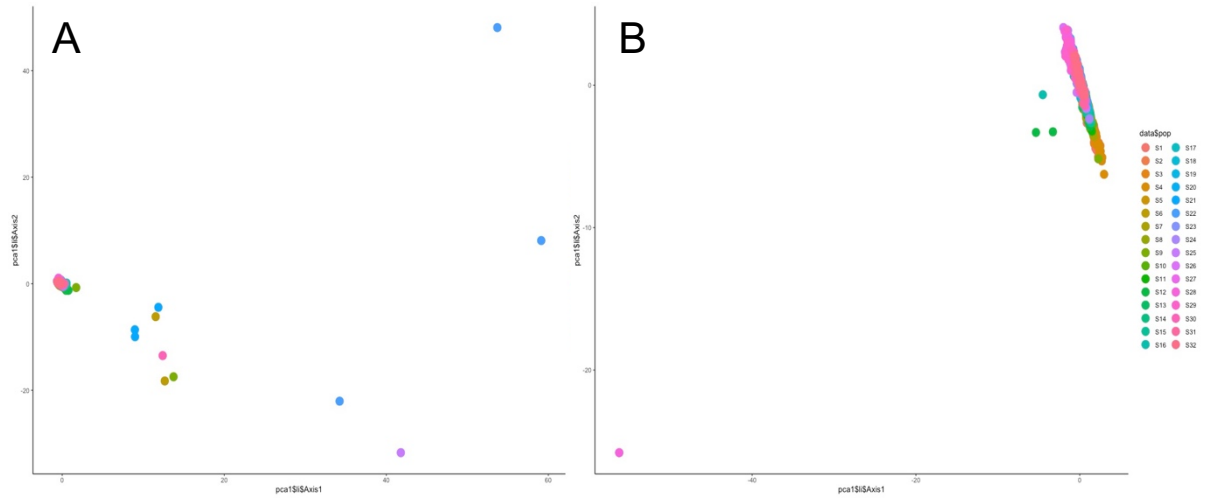

Figure S1. A. The PCA ran on the whole dataset enabled to identify 11 outliers: S6 (2 ind.), S9 (1 ind.), S21 (3 ind.), S22 (3 ind.), S25 (1 ind.) and S30 (1 ind.). **B**. The PCA ran on the dataset after taking the 11 outliers identified previously enabled to identify another outlier coming from S28.

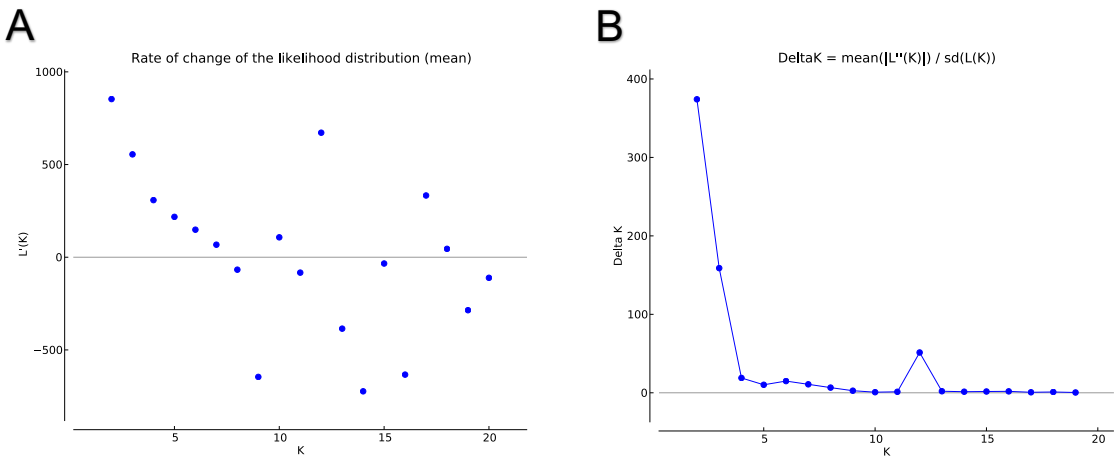

Figure S2. **A**. Rate of likelihood distribution (Pritchard & Wen 2003) and **B**. Delta K method (Evanno et al. 2005) associated to the STRUCTURE analyses.